PROCEEDINGS, 48th Workshop on Geothermal Reservoir Engineering
Stanford University, Stanford, California, February 6-8, 2023
SGP-TR-224

Closed-loop Geothermal Working Group Study - Understanding Thermal Performance and Economic Forecasts via Numerical Simulation

Mark White[1], Mario Martinez[2], Yaroslav Vasyliv[2], Koenraad Beckers[3], Gabriela Bran-Anleu[2], Carlo Parisi[4], Paolo Balestra[4], Roland Horne[5], Chad Augustine[3], Laura Pauley[6], Giorgia Bettin[2], Theron Marshall[4], and the Closed Loop Geothermal Working Group

[1]Pacific Northwest National Laboratory, Richland, WA 99352, USA

[2]Sandia National Laboratories, Albuquerque, NM 87155, USA

[3]National Renewable Energy Laboratory, Golden, CO 80401, USA

[4]Idaho National Laboratory, Idaho Falls, ID 83415, USA

[5]Stanford University, Stanford, CA 94305-2004, USA

[6]Pennsylvania State University, University Park, PA 16802, USA

E-mail address, mark.white@pnnl.gov

Keywords: closed-loop geothermal, numerical simulation, techno-economic analysis, Levelized Cost of Heating (LCOH), Levelized Cost of Electricity (LCOE), subcritical-water temperature regime, water working fluid, supercritical CO_2 working fluid, u-shaped configuration, coaxial configuration, Geothermal Data Repository (GDR), case studies, code comparison, collaborative study

ABSTRACT

The Closed Loop Geothermal Working Group is a collaborative study, funded by the United States Department of Energy (DOE), Geothermal Technologies Office (GTO) to understand the potential and limitations of producing thermal and mechanical energy from geothermal reservoirs closed-loop systems (i.e., marginal working fluid losses). In this study, teams of scientists and engineers from four national laboratories, plus expert panel members are applying numerical simulators and analytical tools to model heat recovery from closed-loop geothermal systems and then subsequently using outlet temperature and pressure versus time from these models to forecast two economic indicators: 1) Levelized Cost Of Heating (LCOH) and 2) Levelized Cost Of Electricity (LCOE), over a range of drilling costs. Numerical simulators and analytical tools applied in the study, including those for technical and economic analyses, were those developed by the participating institutes, yielding independent calculations of energy production and economic forecasts, increasing confidence in the analysis. The study was designed to investigate an array of system configurations, working fluids, geothermal reservoir characteristics, operational periods, and heat transfer enhancements. During the opening year of the study the focus was on water as the working fluid in the closed-loop systems that either had a u-shaped or coaxial configuration. The principal objectives during the opening year were to determine upper limits for thermal and mechanical energy recovery and optimal operational and configuration parameters for each scenario, and to understand the limiting factors to system performance. One important outcome from the first year of the study was that simulation results from models using simple discretizations in a radial direction (i.e., axisymmetric models) to the borehole compared favorably with more conventional numerical simulations with fine discretizations around the borehole and embedded borehole modeling approaches. Moreover, the axisymmetric models compared well with available field observations and analytical models and were shown to be numerically efficient. During the second year of the study, a database comprising 2.4 million simulation scenarios was created of closed-loop system performance in terms of production temperature and pressure versus time, across nine scenario parameters: 1) water and supercritical CO2 (scCO2) working fluids, 2) u-shaped and coaxial configurations, 3) mass flow rate, 4) thermal conductivity, 5) geothermal gradient, 6) vertical depth, 7) horizontal extent, 8) inlet temperature, and 9) borehole diameter. LCOH and LCOE were then computed for each of the 2.4 million scenarios across a range of drilling costs. For the LCOE, electricity generation was computed using an Organic Rankine cycle (for water) or direct turbine expansion cycle (for scCO2). The database is stored in a Hierarchical Data Format (HDF5) file structure that will be available on the Geothermal Data Repository (GDR). A companion paper describes methods for extracting information from the database via Python scripts and the execution of economic analysis. This paper provides an overview of the Closed-loop Working Group study, including key outcomes from first and second years and discussion of optimal configurations with respect to LCOH and LCOE over a range of drilling costs.

1. INTRODUCTION

Deep geothermal systems designed to extract thermal energy at the commercial scale for applications, such as district heating, industrial process heating, and electricity generation. Commercials-scale operations are necessitated by the capital and operating costs associated with accessing thermal energy kilometers beneath the earth's surface. Hydrothermal systems extract thermal energy by producing water from hot rock with ample intrinsic permeability (hot wet rock (HWR)), enhanced geothermal systems (EGS) extract thermal energy from hot rock with insufficient intrinsic permeability for producing water (hot dry rock (HDR)) by creating permeability through fracture stimulation (Brown et al., 2012). In contrast, closed-loop geothermal systems (CLGSs) extract thermal energy from either HWR or HDR reservoirs by circulating a working fluid through a system of sealed boreholes originating and terminating at the ground surface, and passing through either HDR or HWR. Whereas a multitude of subsurface borehole trajectories are conceivable, two basic configurations

exist: 1) u-shaped and 2) coaxial (Fig. 1). In the u-shaped configuration the borehole inlet and outlet collars are separate, and in the coaxial configuration the inlet and outlet fluids are separated within a single collar via coaxial tubing. For HDR, thermal conduction is the sole heat transport mechanism by which energy is transferred from the rock to the borehole exterior. For HWR, natural convection and thermal conduction heat transport mechanism are active. For more than four decades, numerical simulations (Bodvarsson et al., 1985) have been used to compute extracted thermal energy versus time from hydrothermal, EGS, and CLGSs. Compared with CLGSs, heterogeneities in HWR intrinsic permeability and HDR fracture configurations make the uncertainties in the calculations greater for hydrothermal and EGS systems.

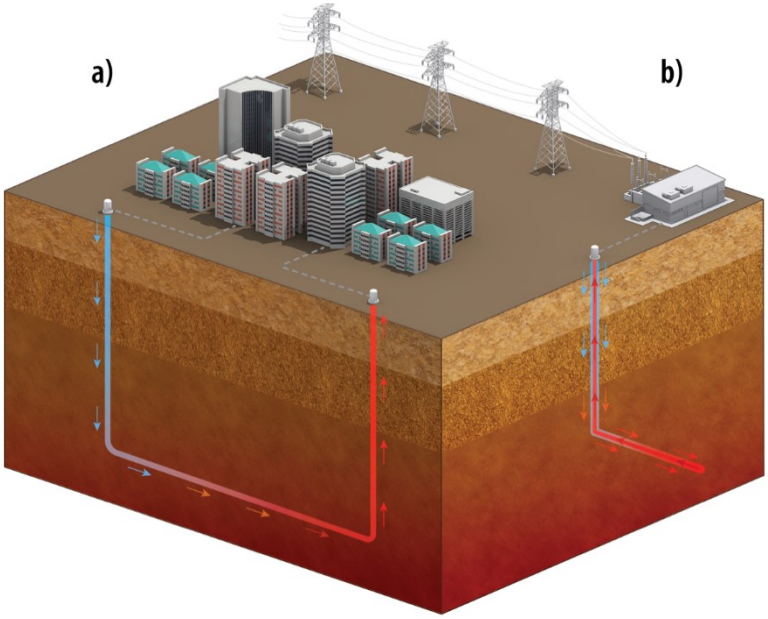

Figure 1: Two common types of closed-loop geothermal systems are a) u-shaped design (with one or multiple laterals) and b) co-axial design or "pipe-in-pipe"-configuration. Photo credit: NREL.

For CLGSs in HDR a number of analytical solutions have been developed to quantify the transfer of heat between the earth and working fluid. Ramey (1962) developed a simple algebraic form to estimate the temperature of working fluid, casing, and tubing as a function of depth and time, using the assumptions that heat transfer within the borehole under steady-state conditions and heat transfer between the earth and borehole follows unsteady radial conduction. The Ramey model is appropriate for analyzing u-shaped configurations. Hagoort (2004, 2005) published corrections to the Ramey (1962) solution for the early transient period, with the boundary for the early transient period being defined by

$$t_{Fo} < N_{Gz}; \quad t_{Fo} = \frac{\alpha\, t}{r_2^2}; \quad N_{Gz} = \frac{\alpha\,(L_1+L_2+L_1)}{r_1^2\, u} \tag{1}$$

where t_{Fo}, N_{Gz}, α, t, r_1, r_2, L_1, L_2, and u are Fourier time, Graetz number, thermal diffusivity of the rock (m^2/s), time (s), hydraulic radius (m), borehole radius (m), vertical length (m), horizontal length (m), and flow velocity (m/s). For typical CLGSs, where the rock thermal diffusivity is on the order of 10^{-6} m^2/s, borehole radius is greater than 0.1 m, fluid velocity is greater than 0.16 m/s, and vertical and horizontal lengths are on the order of kilometers, a representative upper limit for the Graetz number is roughly 10, which equates to roughly one month of time. Whereas the classical Ramey solution (1962) was created to predict the change in fluid temperature of high-temperature fluids for enhancing oil recovery, it provides a clear demonstration of the importance of thermal conductivity for CLGSs. The outlet temperature of a u-shaped closed loop geothermal system is shown in Fig. 2 at the outlet of the downward, horizontal and upward legs for bulk rock thermal conductivities of 3 and 10 W/m K, with the 3 W/m K value being more typical. Production temperatures at 40 years at the surface of roughly 130˚C for a rock thermal conductivity of 3 W/m K sharply contrast with the 210˚C temperatures computed for a rock thermal conductivity of 10 W/m K, with all other parameters being identical. The thermal conductivity of dense igneous and metamorphic rocks at 30˚C are within the 1.0 to 4.0 W/m K range, and thermal conductivity generally sharply declines with temperature over the range from 30 to 300˚C (Robertson, 1988). Since heat transfer in this system is dominated by conduction through the rock, a u-shaped CLGS will always have production temperatures well below the reservoir temperature over its useful lifetime. Enhanced geothermal systems overcome the deficits associated with rock thermal conductivity via surface area contact between the working fluid and rock volume. For closed-loop geothermal, surface area increases are achieved principally through extending the overall horizontal distance of either single or multiple laterals. For example, using the three-stage Ramey solution, as before with a rock thermal conductivity of 3.0 W/m K, outlet temperatures similar to those computed for a rock thermal conductivity of 10.0 W/m K, are achievable with a horizontal extent of 10.0 km.

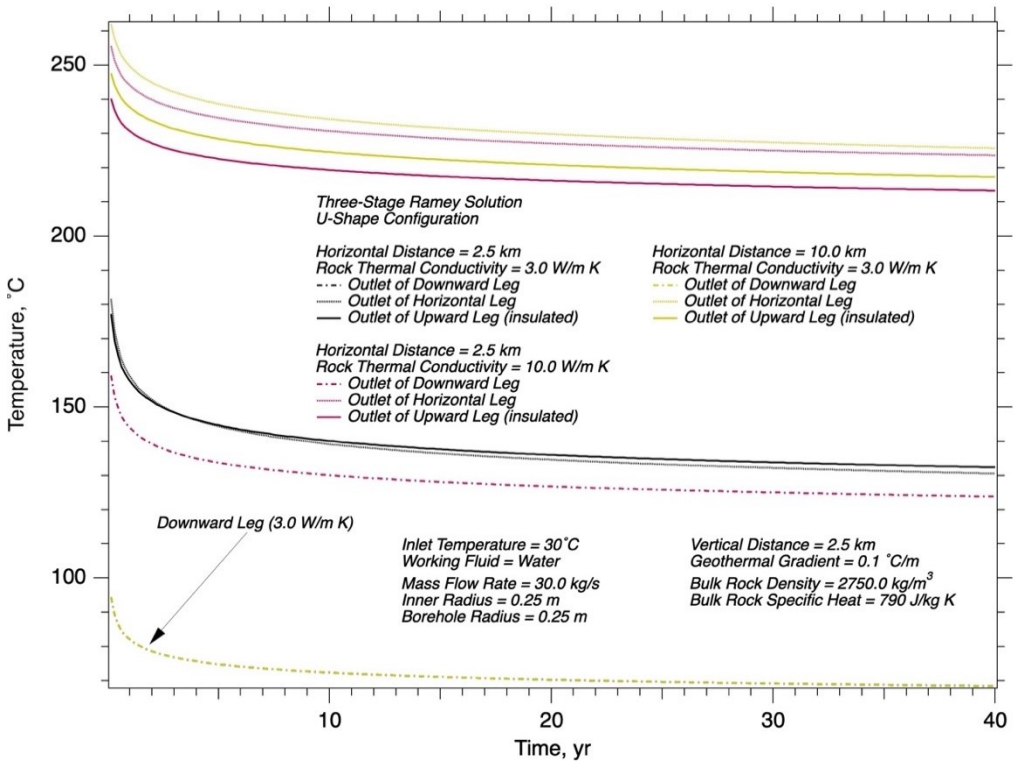

Figure 2: Ramey's solution for outlet temperatures at three stages of a u-shaped configuration for a rock thermal conductivity of 3.0 and 10.0 W/m K at horizontal lengths of 2.5 km and 10.0 km, for a bottom-depth temperature of 275°C.

Horne (1980) developed an analytical model for computing the thermal performance of CLGSs with a coaxial configuration, allowing for downward flow in either the center tube or annulus. Horne's solution expresses the variation of the over-all heat transfer coefficient between the inside of the annulus and earth via an inverse Laplace transform, in contrast to the Ramey (1962) solution, which makes use of a dimensionless time function, which is approximated with a function of the outer tube radius, rock thermal diffusivity and time. Regardless of the solution approach or configuration of the geothermal closed-loop system, the characteristics of the outlet temperature versus time plots are consistent – a transient period, early in time, with a sharp decline in temperature, followed with a slower decline in temperature. The inverse Laplace transform of the Horne solution is a function of the Laplace transform variable (i.e., inverse time), outer tube radius, rock diffusivity, and rock thermal conductivity. The outlet temperature of a geothermal closed-loop system in a coaxial configuration is shown in Fig. 3 for three scenarios: 1) vertical length of 3.5 km, bulk rock thermal conductivity of 3.0 W/m K, 2) vertical length of 3.5 km, bulk rock thermal conductivity of 10.0 W/m K, and 3) vertical length of 10.0 km, bulk rock thermal conductivity of 3.0 W/m K. The geothermal gradient was adjusted to maintain the rock temperature at the bottom of the loop. As with the classical Ramey solution for the u-shaped configuration, the outlet temperature for a typical rock thermal conductivity of 3.0 W/m K (Robertson, 1988) at 3.5 km length was 75.3°C at 40 years. An outlet temperature of 124.8°C was computed for a rock thermal conductivity of 10.0 W/m K, with all other parameters being identical, but this thermal conductivity is outside of the range reported by Robertson (1988) for dense igneous and metamorphic rocks. Similar outlet temperatures can be achieved with a rock thermal conductivity of 3.0 W/m K, but requires an overall borehole length of 10 km, as shown in Fig 3. For both the u-shaped and coaxial configurations, bulk rock thermal conductivity, thermal diffusivity and surface area, as created through borehole radius and length, are the critical parameters defining outlet temperatures of CLGSs. Horne's solution (1980) expresses the variation of the over-all heat transfer coefficient between the inside of the annulus and earth via an inverse Laplace transform, in contrast to the Ramey (1962) solution, which makes use of a dimensionless time function, which is approximated with a function of the outer tube radius, rock thermal diffusivity and time. Regardless of the solution approach or configuration of the geothermal closed-loop system, the characteristics of the outlet temperature versus time plots are consistent – a transient period, early in time, with a sharp decline in temperature, followed with a slower decline in temperature.

The foundation work of Ramey (1962) and Horne (1980) provide insight as to the critical parameters controlling the performance of CLGSs, with respect to the quality and quantity of recovered heat; however, they do not handle alternative working fluids (e.g., sCO2) and don't consider design options or the economics of the produced heat, in terms of the costs for direct use or electricity generation. To objectively address these factors, the United States Department of Energy (DOE), Geothermal Technologies Office (GTO), funded a working group comprising teams of scientists and engineers from four national laboratories and an expert panel to study, via numerical simulation the techno-economic performance of CLGSs. During the first stage of this study, teams from the national laboratories (Idaho National Laboratory (INL), National Renewable Energy Laboratory (NREL), Pacific Northwest National Laboratory (PNNL) and Sandia National Laboratories (SNL), applied independent numerical simulators to compute the thermal performance (i.e., outlet temperature versus time and produced thermal power versus time) for u-shaped and coaxial system configurations in both hot-dry and hot-wet rock reservoirs, but restricted to water as the working fluid. The INL and PNNL teams applied their coupled subsurface flow and heat transport

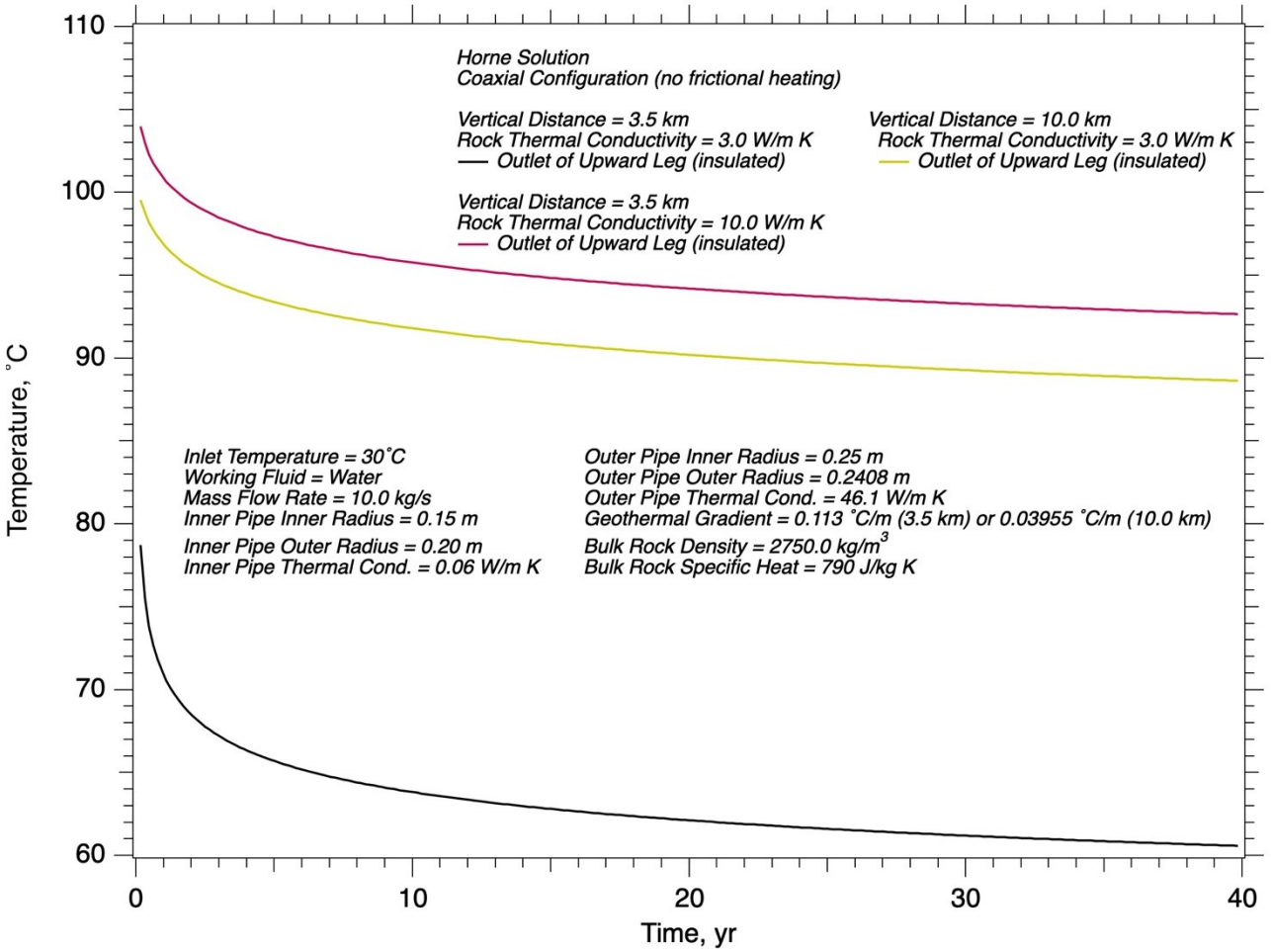

Figure 3: Horne's solution for outlet temperatures for a vertical coaxial configuration for a rock thermal conductivity of 3.0 and 10.0 W/m K at overall lengths of 3.5 and 10.0 km, with identical bottom-depth temperatures of 300˚C.

simulators, with either integrated or coupled borehole modeling, whereas the SNL and NREL teams both used axisymmetric models coupled to 1D area averaged fluid models. Results from the first stage of the study revealed that both the coupled subsurface flow and heat transport simulator and axisymmetric modeling approaches compared well with available field data and via intercomparisons for scenarios without field data (White et al., 2021; Parisi et al., 2021; Vasyliv et al., 2021; Beckers et al., 2022). During the second stage of this study, system enhancements, alternative working fluids, specific case studies, and the impacts of natural convection were considered, all using numerical simulation. Additionally, a database comprising both thermal performance and economic analyses across seven parameters for a hot-dry-rock reservoir was developed, along with scripts and web-based interfaces to access this database. Two companion papers to this study overview paper are published in the proceedings of this 48th Workshop on Geothermal Reservoir Engineering. The first paper (Parisi et al., 2023), describes the application of the INL developed coupling of the RELAP5-3D and FALCON simulators to specific case studies, and the second paper (Beckers et al., 2023) describes the techno-economic database and techniques for reading, visualizing, and querying quantities of interest using Python scripts and associated web-based interfaces. This paper provides and overview of the axisymmetric modeling approach used to develop the thermal component of the developed database, analyzes the technical and economic elements of the developed database, discusses the thermal performance impact of oversized boreholes and natural convection on CLGSs, and provides conclusions on thermal performance and economic realities of CLGSs for hot-dry-rock reservoirs with temperatures below the critical point of water (i.e., 374˚C).

2. SUBSURFACE MODELING APPROACHES AND COMPARISONS

During the first stage of this study, the thermal performance of two CLGSs, a u-shaped borehole in a hot-dry-rock (HDR) reservoir and a coaxial borehole in a hot-wet-rock reservoir, were computed using three independent modeling approaches and computer codes: 1) PNNL's STOMP-GT simulator with its embedded borehole and fracture capabilities (White et al., 2020), 2) INL's coupled RELAP5 and 3D-PRONGHORN computer codes (Parisi et al., 2021), and 3) SNL's model (Vasyliv et al., 2021), developed using SNL's multi-physics Sierra computer code (Team, 2020). The u-shaped configuration in a hot-dry-rock reservoir scenario was based on reservoir parameters from Utah FORGE, an initiative funded by the U.S. Department of Energy (DOE) for research and development of enhanced geothermal systems (EGS). The borehole trajectory comprised two vertical sections connected to a 10 km horizontal section at a depth of 2539 m (bgs), at a temperature of approximately 200˚C, with deviation rate between vertical and horizontal of 5˚/100 ft (0.164˚/m). Thermal, geomechanical, and fracture properties for the granitoid reservoir were determined from field and laboratory measurements and modeling

calibrations (Podgorney et al., 2020), which included a rock bulk thermal conductivity of 3.05 W/m K, bulk specific heat of 790.0 J/kg K, bulk density of 2750.0 kg/m^3, and geothermal gradient of 0.079 ˚C/m. The working fluid is liquid water and the heat transfer between the inner surface of the pipe casing follows the correlation of Gnielinski for turbulent flow (Gnielinski, 1975; Incropera and DeWitt, 2007), which is valid for the range of Prandtl and Reynolds numbers from $0.5 \leq Pr \leq 2{,}000$ and $3{,}000 \leq ReD \leq 5{,}000{,}000$. The outlet pressure is held to maintain liquid water conditions. The system is to be independently optimized for cumulative thermal or mechanical energy via three independent parameters: 1) horizontal extent (i.e., spacing between vertical legs of the boreholes, 2) flow rate, and 3) insulation length on the ascending vertical leg. Heat loss through the insulated section was assumed to be negligible. The inlet temperature was fixed at 30˚C.

The coaxial configuration in a hot-wet-rock (HWR) reservoir scenario was based on the field experiments of Morita et al. (1992a; 1992b), involving the testing of a downhole coaxial heat exchanger were conducted in the upper 879.6 m length of the HGP-A well on the island of Hawaii, just south of Puu Honuaula. This University of Hawaii (UH) drilled geothermal well produced 12.6 kg/s with nearly equal amounts of liquid and steam at a surface temperature of 186˚C and operated a 2.8 MW electric plant from 1981 to 1989. Lava from the Kilauea 2018 eruption buried the site. Two problem scenarios were developed for this site for a coaxial closed-loop system configuration: 1) validation study of the experiment, 2) extension of the coaxial system to the bottom of the HGP-A well. The porosity and intrinsic permeability of the host rock at the Puu Honuaula site allowed for water circulation in contrast to the nearly impermeable rock of the Utah FORGE site, which distinguishes hot-wet-rock from hot-dry-rock. Key thermal and hydrologic properties of the reservoir included a grain thermal conductivity of 3.02 W/m K, porosity of 0.133, grain specific heat of 965.0 J/kg K, grain density of 3000 kg/m^3, geothermal gradient of 0.112, and intrinsic permeability of 10^{-12} m^2. The experimentally measured geothermal gradient was nonlinear, which required consideration in modeling early outlet temperatures, and an effective rock thermal conductivity of 1.44 W/m K was determined by Morita et al. (1992a; 1992b). The well configuration for the first scenario was identical to that for the experiment (Morita et al., 1992a; 1992b), with cement filling the space between the upper-cased sections of the well. Properties of the well materials, including those for the steel casing, cement, and insulated inner pipe, which was constructed as specified by Morita et al. (1988), with a density of 3925 kg/m^3, specific heat of 235 J/kg K, and thermal conductivity of 0.07 W/m K. The second scenario (i.e., extended configuration), used a modified version of the actual experiment, sizes of the coaxial pipes being increased, but with area ratios between the inner pipe and outer annular space maintained to those of the experiment (i.e., 0.108). This area ratio was designed to increase the residence time of the water in the outer annular space and minimize the residence time in the upward leg. The third scenario (i.e., deviated well configuration) used the upper well configuration of the second scenario, to a depth of 2189.73 m (bgs), then deviated at a rate of 5˚/100 ft (0.164˚/m) until horizontal (depth of 2539.01 m (bgs)), then extended horizontally 5 km. The working fluid is liquid water and the heat transfer between water and pipe walls follows the correlation of Gnielinski for turbulent flow (Gnielinski, 1975; Incropera and DeWitt, 2007).

The INL team solved the u-shaped HDR and coaxial HWR CLGS problems using a combination of two proven computer codes, the RELAP5-3D code (Team, 2018a; 2018b) to compute thermal and hydraulic processes inside the flow tubes and the PRONGHORN computer code (Novak et al., 2021) to compute the thermal and hydrologic processes in the subsurface outside of the flow tubes. PRONGHORN received heat flux and fluid temperature from RELAP5-3D and sent wall temperatures to RELAP5-3D. Coordination of the two computer codes was via Python scripts. Three coupling algorithms were used during the study: 1) sequential explicit, 2) implicit with Picard iteration, and 3) implicit with Newton-Raphson iteration. RELAP5-3D is a nuclear system thermal-hydraulic code that is part of the RELAP5 codes family developed for light-water reactor transient analysis. RELAP5-3D is based on nonhomogeneous and nonequilibrium model for the two-phase system that is solved by a fast, partially implicit numerical scheme (semi-implicit and nearly implicit) to permit economical calculations of system transients. Solving a 6-equation model (mass, momentum and energy conservation equations for both liquid and vapor phases) allows RELAP5-3D to calculate in every node/junction of the discretized system water and steam velocities and temperatures. The pressure of both phases is assumed to be identical. PRONGHORN code is a porous media approach code which can simulate three-dimensional one-phase flows, heat convection and heat conduction phenomena. The code is part of the INL' MOOSE computational framework and it has been used for simulating complex flow patterns and heat transfer for the high-temperature gas reactors. The code is solving the one-phase mass, momentum and energy conservation equations and the energy transfer using an implicit numerical scheme. Finite elements (FE) and finite volumes meshing scheme can be employed, giving to the code the possibility of simulating also complex three-dimensional geometries.

The PNNL team solved the u-shaped HDR and coaxial HWR CLGS problems using its STOMP-GT (Subsurface Transport Over Multiple Phases – GeoThermal) reservoir simulator, an operational mode of the STOMP suite of simulators (Oostrom and White, 2004). STOMP-GT solves conservation equations for water mass, air mass, salt mass and energy, with capabilities for modeling coupled geochemical processes via its ECKEChem module and coupled porothermoelastic geomechanics via its finite-element based GeoMech module. The STOMP-GT simulator solves governing conservation equations and associated constitutive equations for multifluid flow and transport via the finite-volume approach, with backward Euler time discretization, and Newton-Raphson iteration to resolve nonlinearities. The computational domain is based on hexahedra grid cells, yielding structured boundary fitted discretization of the rock matrix. Embedded fractures and boreholes were incorporated into the simulator as additional finite-volume grid cells. Boreholes are defined by piece-wise trajectories and radii, following the well models developed for the STOMP-CO2 simulators (White et al., 2013). This three-domain approach yields a Jacobian matrix which is banded within the rock matrix equations with a seven-point stencil of 4x4 blocks (i.e., water mass, air mass, salt mass, and energy), banded within the fracture equations with a four-point stencil of 4x4 blocks, and banded within the borehole equations with a three-point stencil of 4x4 blocks. The inter-domain connections yield additional 4x4 blocks via the transfer terms between the three domains: fractures-rock matrix, boreholes-rock matrix, and fractures-boreholes, conserving component and tracer mass and energy. The central concept for this mathematical modeling approach is that fractures and boreholes are embedded in the matrix grid structure, that is no attempt is made to alter the matrix grid structure with respect to the embedded fractures and boreholes. This assumption, therefore, allows for single fracture triangles to intersect multiple matrix grid cells and multiple fracture triangles to intersect single matrix grid cells. Boreholes are specified via three-dimensional piece-wise trajectories through the rock matrix domain, with each

piece of the trajectory being defined by a starting and ending coordinate location in the global coordinate framework. Borehole trajectories are discretized into borehole nodes; where, borehole nodes are defined as linear sub-sections of the borehole trajectory. Borehole nodes start and end at either the point at which the borehole trajectory intersects a matrix grid cell surface or at the starting or ending point of a borehole interval. Fluid flow between a borehole node and rock matrix grid cell is modelled with a modified Peaceman well index formulation. The modification, known as the projection well index (Shu, 2005), involves the projection of the linear well interval segments onto the principal orthogonal axes of the computational grid.

The SNL team developed simplified models (Vasyliv et al. 2021) using the thermal-fluids code Aria (Team, 2020). For the HDR scenarios, a 1D area averaged thermal energy equation was coupled through convective flux boundary conditions to 2D axisymmetric transient heat conduction domains as shown in Fig. 4. For the HDR systems, the following modeling assumptions were made: 1) the formation heat conduction at the interface between region 1-2 and region 2-3 is negligible, 2) a 2D axisymmetric assumption is valid in each region, 3) the horizontal formation has a constant initial temperature corresponding to the temperature at the maximum borehole depth, and 4) the "elbow" sections of the U-tube (see Fig. 4) can be ignored as the difference in surface area in contact with the formation is negligible compared to the rest of the U-tube. Assumptions 2 and 3 were verified using a 3D model of the formation, showing a negligible impact of the geothermal gradient on the horizontal leg. Adiabatic boundary conditions are applied to the remaining formation boundaries and the formation outer radius is set to 150 m. This formation radius was sufficient to enclose the thermal drawdown from energy extraction at the borehole. A similar axisymmetric modeling approach was used for the coaxial HDR version of this problem, as shown in Fig. 5. Lastly, for the HWR version, the formation was instead modeled with a 2D axisymmetric coupled heat and mass transport model, that included buoyant convection currents induced by cooling of formation waters near the borehole.

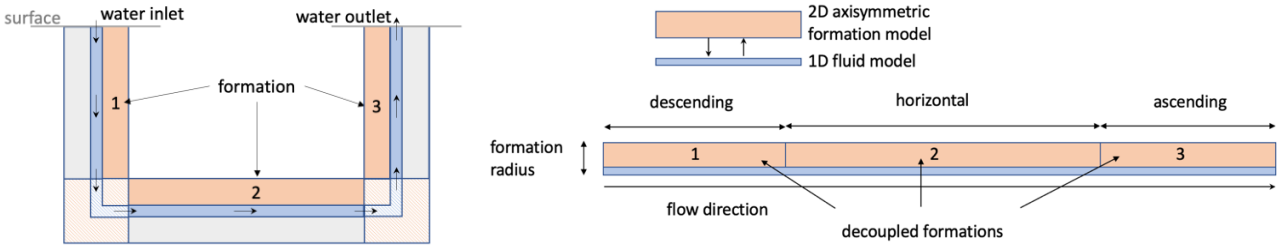

Figure 4: (left) SNL computational model for the u-shaped HDR problem, (right) SNL 2D axisymmetric model for the U-tube closed loop geothermal systems. The mesh (not shown) is biased towards the borehole to resolve the radial temperature gradients. While the formations are assumed to not directly interact, all three formations are still coupled to each other through the heat exchange with the 1D fluid model.

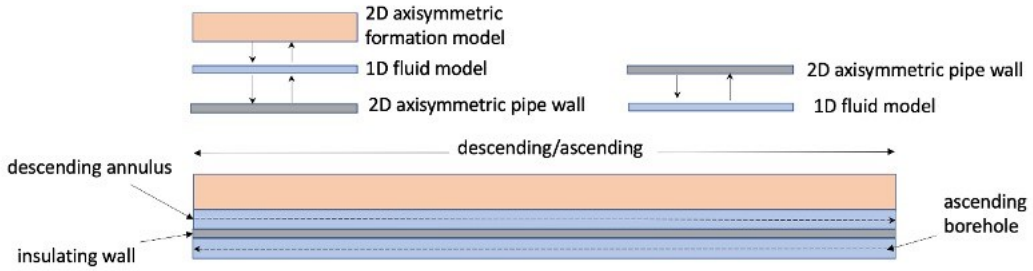

Figure 5: SNL coaxial heat exchanger computational model.

With respect to the first stage of the study, the principal objective of the u-shape HDR problem was to optimize the design with respect to an objective function for both mechanical and thermal energy production over a 40-year system life, considering drilling costs of $0/m, $500/m, $1000/m, and $1500/m. The results of this analysis were reported in White et al. (2021), along with the objective functions, but more importantly for the second stage of the study, a comparison of outlet temperature versus time for two scenarios among two analytical solutions (noted as NREL and Stanford), and two numerical simulation solutions (noted as PNNL and SNL) are shown in Fig. 6. The agreement in results provide evidence for the validity of the assumptions and axisymmetric modeling approach used by SNL and the analytical models. Similarly, as shown in Fig. 7, both SNL's modeling approach as well as INL's approach were able to reproduce the experimental results of Morita et al. (1992a) (Scenario 1). Note that for Scenario 1, no attempt was made to simulate the natural convection over the short seven-day period of the experiment. Instead, the problem was simulated using HDR models with Morita's reported effective thermal conductivity. Comparison of PNNL and SNL simulation results for the coaxial HWR problem (Scenario 2) additionally showed close comparisons for outlet temperature, as shown in Fig. 8.

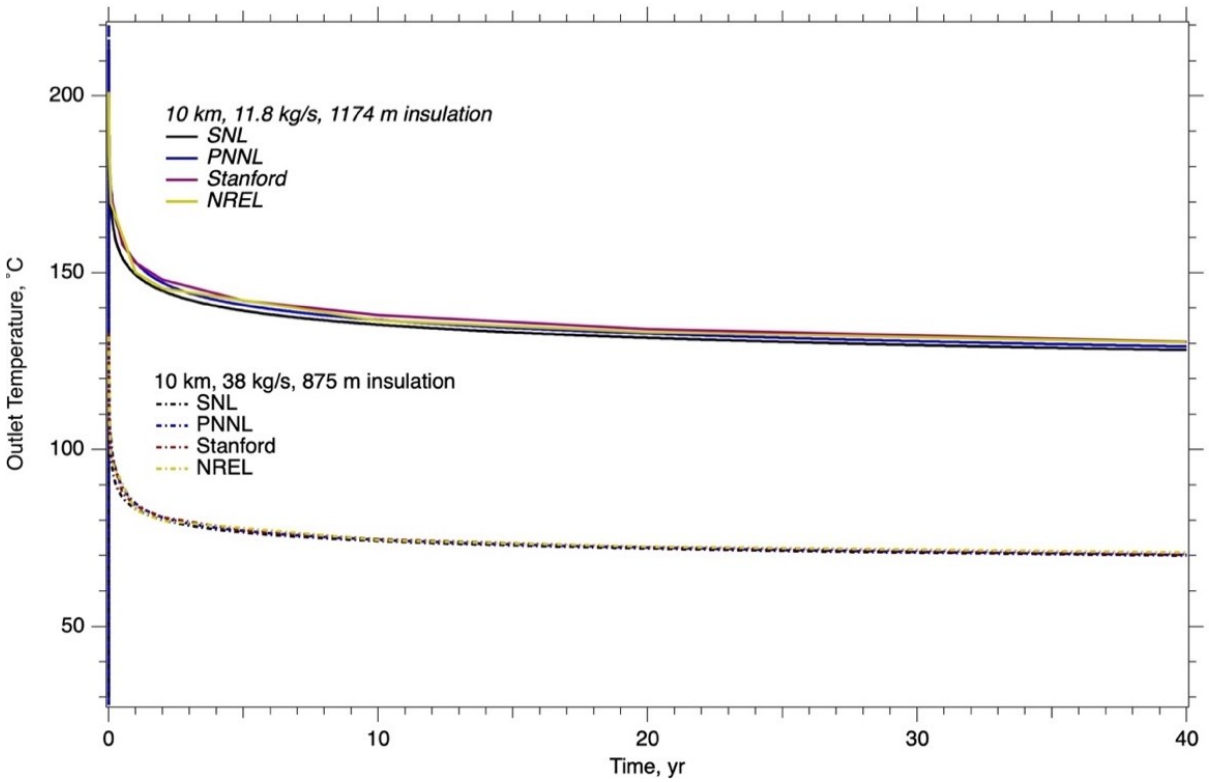

Figure 6: Comparison of outlet temperature versus time across numerical simulations and analytical solutions for optimal solutions of the energy objective functions at zero drilling costs for the u-shaped HDR problem.

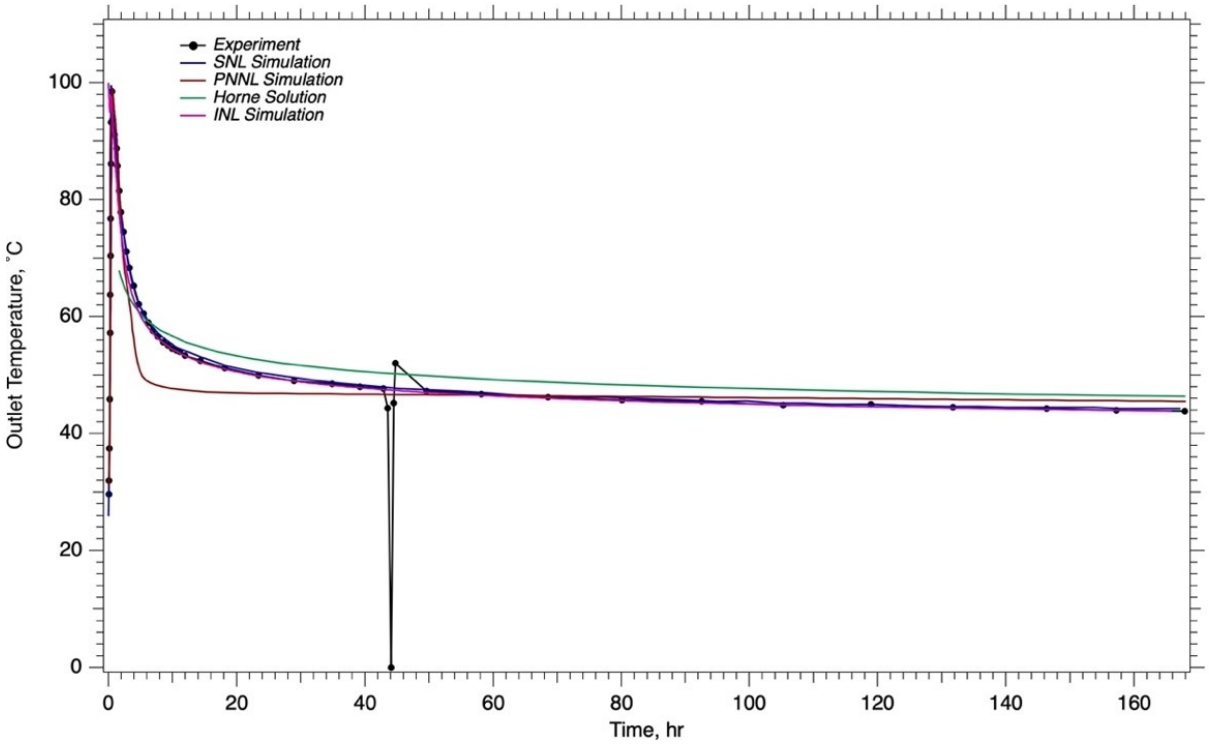

Figure 7: Comparison of outlet temperature versus time across numerical simulations and analytical solutions for the coaxial HWR problem (Scenario 1).

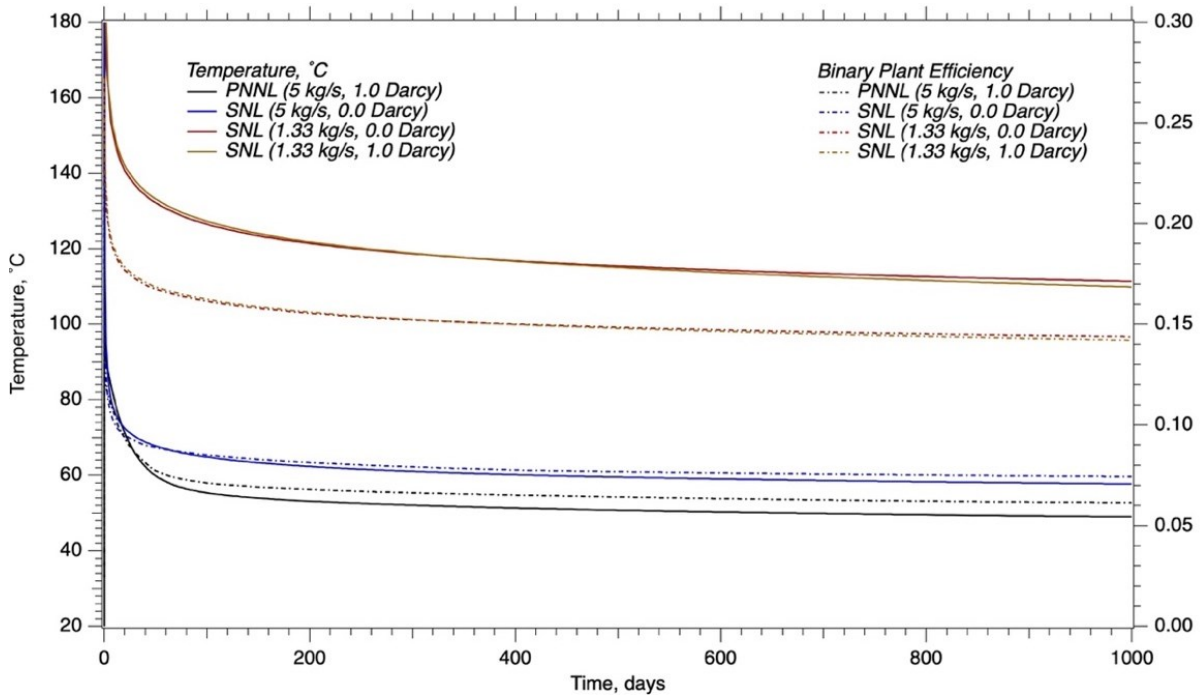

Figure 8: Comparison of outlet temperature and binary plant efficiency versus time across numerical simulations for the coaxial HWR problem (Scenario 2).

Although not formally a component of the first stage of the study the NREL team was concurrently investigating the performance of both coaxial and u-shaped CLGSs, including horizontal extensions for the coaxial configuration and multiple laterals for the u-shaped configuration (Beckers et al., 2022). The study evaluated 34 different scenarios, considering both water and scCO2 as the working fluid, over an operational period of 20 years, with subsurface temperatures ranging from 100 to 500˚C, inlet temperatures from 10 to 40˚C and mass flow rates from 10 to 40 kg/s. As with the subject study, the NREL team used three modeling approaches: 1) commercial finite-element package, 2) Slender-Body Theory (SBT) modeling approach (Beckers et al., 2015), and 3) Ramey's analytical solution (Ramey, 1962). The SBT model is similar to the SNL model; however, heat transfer between the wellbore and rock is modeled via an analytical solution, based on Green's functions. The SBT model was modified for this study to account for coaxial configurations, multiple laterals, and working fluids other than water.

3. DATABASE OF NUMERICAL SIMULATIONS FOR HDR SYSTEMS TO 374˚C

The first stage of the study indicated that 2D axisymmetric coupled modeling approaches were sufficiently accurate for HDR when compared against the more conventional subsurface reservoir modeling approaches and analytical solutions. At the start of second stage of the study, SNL extended their previously developed model to handle scCO2 as a working fluid (see Beckers et al. 2023) and cross-validated their model against NREL's SBT model showing excellent agreement. The principal advantage of the axisymmetric modeling approach is the speed of execution, allowing for the rapid processing of simulations over a 40-year simulation period. With this capability established and access to the high-performance computing facilities at SNL, the project launched a large parametric study involving two system configurations (i.e., u-shape and coaxial) and two working fluids (i.e., water and scCO2) with the assumption of a HDR reservoir, restricted to temperatures below the critical point of water (i.e., 374˚C). The objective for this study was to develop an accessible database that could be used to quickly evaluate the thermal and economic performance of CLGSs that spanned a broad parameter space. Seven variable and nine fixed parameters were selected to describe the geothermal reservoir and system specifications, as shown in Table 1. The total combination of variable parameters yields 631,800 simulations for each combination of system configuration and working fluid, for a total of 2,527,200. Simulations were executed in batches of concurrent runs using the SNL Dakota package (Dalbey et al., 2020). The results were parsed and stored in a single HDF5 file, as described in Beckers et al. (2023). The thermal power production is determined as a function of time as the product of the mass flow rate and the difference in outlet and inlet enthalpy, as computed as a function of temperature and pressure, via the CoolProp package (Bell et al., 2014). Thermal power production is then converted to electrical power production via two methods. When water is the working fluid, heat is converted to electricity using an Organic Rankine Cycle (ORC) power plant on the surface, with the organic fluid optimized for the production temperature. For scCO2 as the working fluid, the fluid directly drives a turbine to generate electricity. These calculations allow for some variability in state conditions during the power cycle, thus allowing for some optimization. In addition to the conversion of heat to electricity, high-level economic assessments were completed to estimate the LCOH and LCOE for the produced heat and electricity, respectively, given drilling costs as described a companion paper (Beckers et al., 2023). The range of rock thermal properties via the classification scheme of Nalla et al. (2005), covers those more favorable for geothermal systems, including the value of 2352.85 J/m2 s1/2 K, reported for The Geysers, California (Barker et al., 1991).

Table 1: Variable and fixed parameters.

Variable Parameters					**Fixed Parameters**		
Description	Bounds	Units	Count		Description	Value	Units
Mass Flow Rate	5 to 100	kg/s	26	mdot	Inlet Pressure	20.0	MPa
Horizontal Extent	1,000 to 20,000	m	20	L2	Ambient Temperature	26.85	˚C
Vertical Depth (bgs)	1,000 to 5,000	m	9	L1	Surface Temperature	25.0	˚C
Geothermal Gradient	0.03 to 0.07	˚C/m	5	grad	Pipe Roughness	0.025	mm
Borehole Diameter	0.2159 to 0.4445	m	3	D	Rock Density	2750	kg/m^3
Inlet Temperature	30 to 60	˚C	3	T_i	Rock Specific Heat	790	J/kg K
Rock Thermal Conductivity	1.5 to 4.5	W/m K	3	k_rock	Inner Pipe / Annulus Area Ratio	1.0	
Rock $\frac{k}{\sqrt{\kappa}}$	1805 to 3127	$J/m^2\ s^{1/2}$ K			Inner Pipe Thickness	0.0192	m
where k is thermal conductivity, κ is thermal diffusivity and $\frac{k}{\sqrt{\kappa}}$ is a thermal characteristic of geothermal rock (Nalla et al., 2005).					Inner Pipe Thermal Conductivity	0.06	W/m K

4. ANALYSES OF TECHNO-ECONOMIC DATABASE FOR HDR SYSTEMS TO 374˚C

The HDF5 files described above and in the companion paper (Beckers et al., 2023) contain a wealth of information about the thermal performance of CLGSs in HDR reservoirs. There are any number of ways in which to make use of these data, such as preliminary assessments of system performance or economic outcomes (via associate Python scripts), or comparison of scenarios or operating parameters, or finding optima. One straightforward use of these data is to understand the impact of individual parameters. For example, consider a u-shaped configuration installed in a geothermal reservoir, with a horizontal extent of 10 km, vertical depth of 2.5 km (bgs), geothermal gradient of 0.065 ˚C/m, borehole diameter of 0.3 m, inlet temperature of 40˚C, and rock thermal conductivity of 3.5 W/m K. The geothermal gradient and vertical depth yield a reservoir temperature of 187.5˚C at the depth of the horizontal run. The outlet temperature and pressure are shown for this system at three mass flow rates and both working fluids in Fig. 9(a) and 9(b), respectively. As anticipated, the outlet temperature is inversely correlated with mass flow rate for both working fluids (i.e., slower moving fluid increases the residence time). The heat transfer coefficient between the working fluid and borehole wall for these simulations was sufficiently high for these simulations to be considered effectively infinite. For example, increasing the coefficient to 1000 W/m^2 K, yielded very slight difference in outlet temperature. Produced energy quality is directly correlated with the outlet enthalpy, or in the case of incompressible fluids, such as water, the temperature. Produced thermal power, however, is the product of outlet enthalpy and mass flow rate, such that the higher outlet temperatures at the lower mass flow rates are offset by the mass flow rate itself, yielding a reversal in results as shown in comparing Fig. 9a and 10a. In converting thermal power to electrical power, however, the produced enthalpy or energy quality becomes important again. The potential electrical power, which was computed via the exergy difference between the outlet and inlet times the mass flow rate (i.e., the availability or maximum work possible), is shown in Fig. 10b. It should be noted that for water, the highest thermal power production occurs at the highest mass flow rate, but this also yields the lowest potential electrical power production, even before consideration of conversion efficiencies, and that the ratio of potential electrical power to thermal power at 40 years is less than 5%.

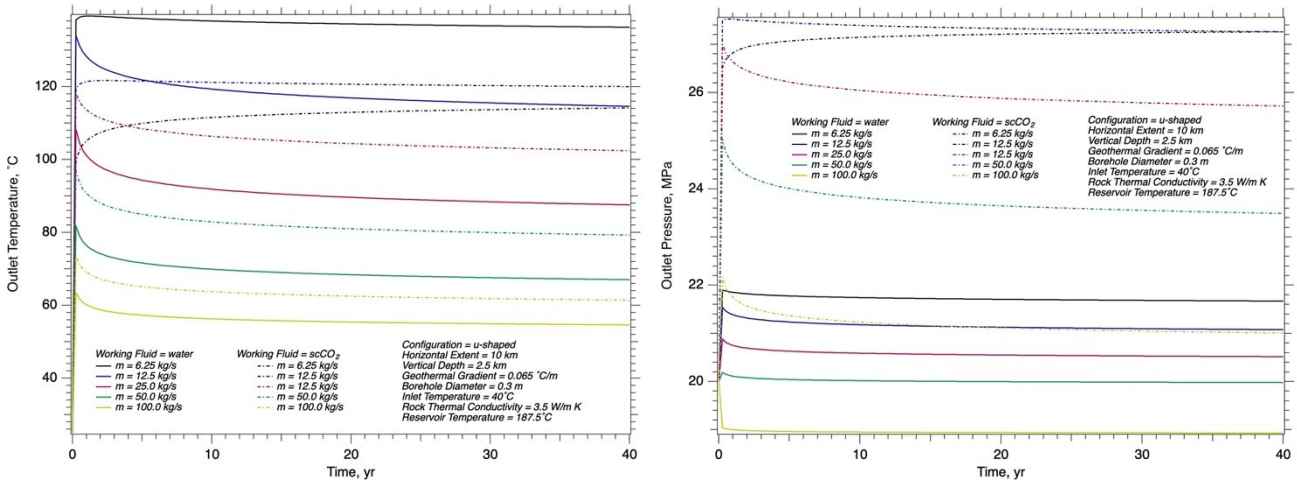

Figure 9: (a) Outlet temperature versus time as a function of mass flow rate and working fluid; (b) Outlet pressure versus time as a function of mass flow rate and working fluid.

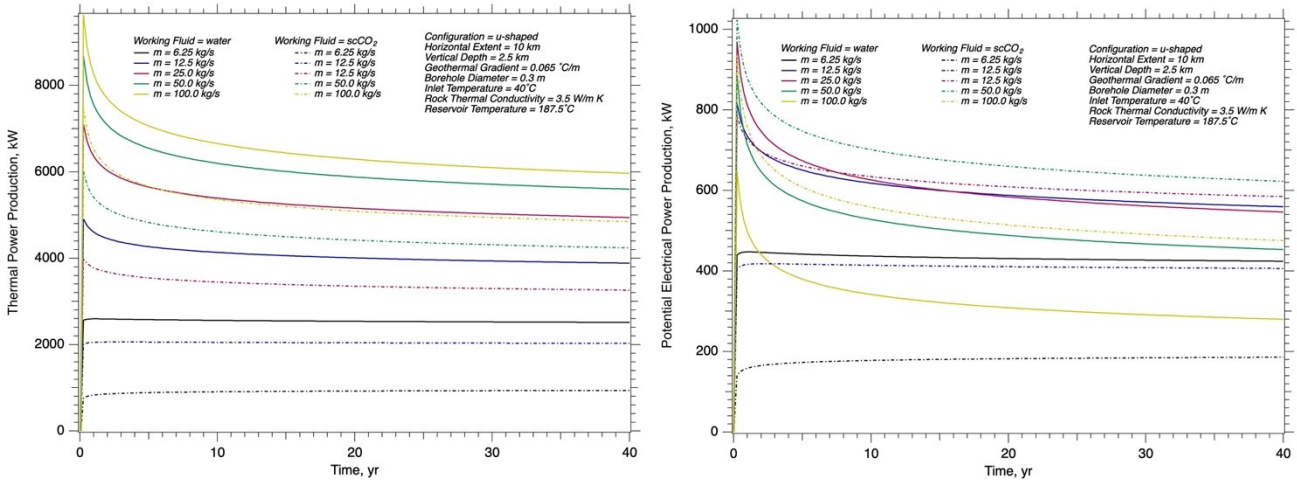

Figure 10: (a) Thermal power versus time as a function of mass flow rate and working fluid; (b) potential electrical power versus time as a function of mass flow rate and working fluid.

Plots of outlet conditions versus time and power production versus time clearly demonstrate the characteristics of radial heat transport, via conduction through the rock to the borehole, which defines the limitations of CLGSs in general. These characteristics are evident in the foundational works of Ramey (1962) and Horne (1980), and in the simulation results from both the classical high-resolution reservoir simulators, and the more recent axisymmetric models. Whereas CLGSs are not limited to the parameters established for this study, it's interesting to investigate the potential and characteristics of CLGSs at the extremes of the parameter set, specified in Table 1. For this example, we will consider a u-tube configuration with $scCO_2$ as the working fluid, with a vertical depth of 5 km (bgs), geothermal gradient of 0.07˚C/m, borehole diameter of 0.4445 m (17.5 in), and inlet temperature of (60˚C). The combination of vertical depth and geothermal gradient yields a temperature of 375˚C for the horizontal run. Three independent parameters will be considered in this example: one reservoir property; rock thermal conductivity, and two engineering parameters; horizontal extent and mass flow rate. Plots of average thermal and potential electrical power production and outlet temperature and pressure are shown in Figs. 11 through 13, for rock thermal conductivities of 1.5, 3.0, and 4.5 W/m K, respectively. This series of plots demonstrates several characteristics of closed-loop systems, in particular for a $scCO_2$ working fluid. Whereas outlet temperatures increase with horizontal extent, maximums are not always associated with lower mass flow rates. Thermal and generally potential electrical power production increase with increasing horizontal extent, mass flow rate and rock thermal conductivity. Optima in potential electrical power production will occur at intermediate flow rates. Moreover, increasing rock thermal conductivity yields higher ratios of potential electrical to thermal power production, moving from 0.259, 0.293, to 0.315 for the three thermal conductivities, shown in the series of plots (i.e., Figs. 11 through 13). Average thermal power production values of 10.9, 17.6, and 22.1 MW_{th} and maximum available power values of 2.8, 5.2, and 7.0 MW_e are at the commercial scale, but achieving those values required drilling 30 km of boreholes - a significant initial capital investment. The question then becomes whether the capital investment is worthwhile, which will be addressed via an economic analysis.

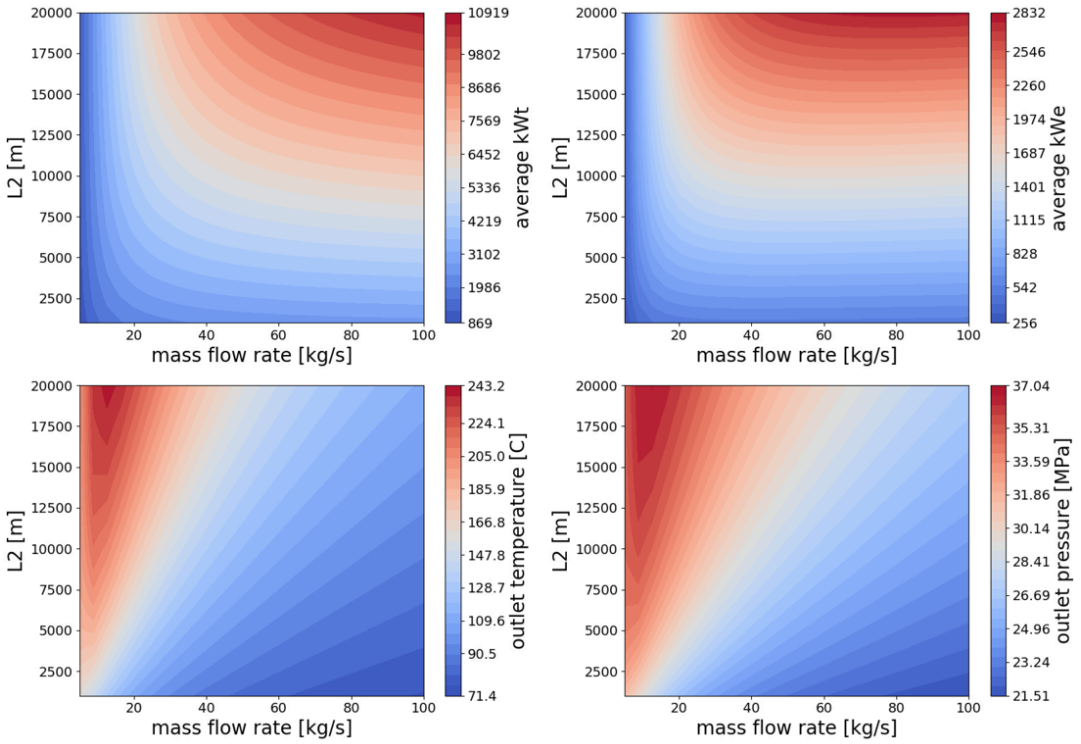

Figure 11: (upper left) Average thermal power production, (upper right) average potential electrical power production, (lower left) outlet temperature, (lower right) outlet pressure versus horizontal extent and mass flow rate at the maximum variable parameters in Table 1 at a rock thermal conductivity of 1.5 W/m K for $scCO_2$ working fluid.

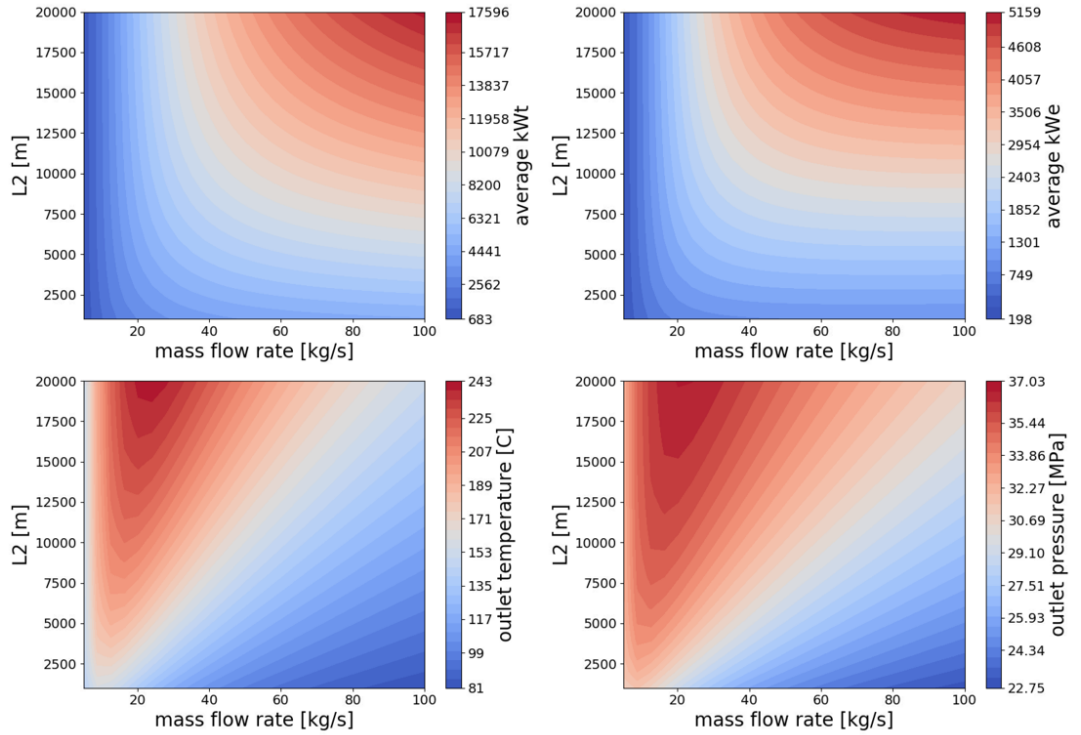

Figure 12: (upper left) Average thermal power production, (upper right) average potential electrical power production, (lower left) outlet temperature, (lower right) outlet pressure versus horizontal extent and mass flow rate at the maximum variable parameters in Table 1 at a rock thermal conductivity of 3.0 W/m K for $scCO_2$ working fluid.

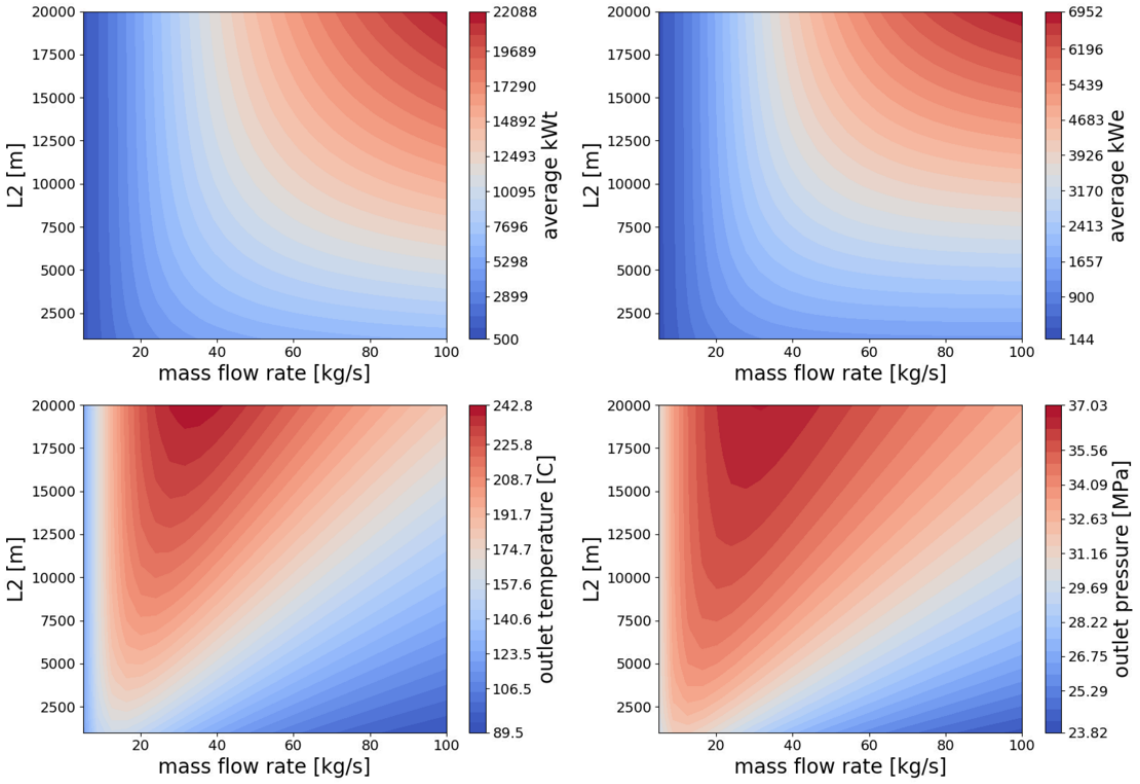

Figure 13: (upper left) Average thermal power production, (upper right) average potential electrical power production, (lower left) outlet temperature, (lower right) outlet pressure versus horizontal extent and mass flow rate at the maximum variable parameters in Table 1 at a rock thermal conductivity of 4.5 W/m K for $scCO_2$ working fluid.

The economic component of this study's techno-economic analysis of CLGS is directed at computing the net average present cost of producing thermal energy (heat) for direct-use applications or generating electricity from the produced heat, using the expressions for levelized cost of heating (LCOH) or levelized cost of electricity (LCOE):

$$LCOH = \frac{sum\ of\ costs\ over\ lifetime}{sum\ of\ heat\ produced} = \frac{\sum_{t=1}^{n} \frac{C_t + O_t}{(1+r)^t}}{\sum_{t=1}^{n} \frac{E_h}{(1+r)^t}} \quad LCOE = \frac{sum\ of\ costs\ over\ lifetime}{sum\ of\ electricity\ generated} = \frac{\sum_{t=1}^{n} \frac{C_t + O_t}{(1+r)^t}}{\sum_{t=1}^{n} \frac{E_e}{(1+r)^t}} \tag{2}$$

where, C_t, O_t, n, r, t, E_h, E_e are capital expenditures (CAPEX) in year t, operating and maintenance expenditures (OPEX) in year t, expected lifetime of the CLGS, discount rate, heat produced in year t, and electricity generated in year t, respectively. Cost correlations for computing LCOH and LCOE are described in a companion paper (Beckers et al., 2023), but it should be noted that the conversion between produced heat and electricity is via a generalized binary organic Rankine cycle for water as the working fluid, limited to temperatures above 100˚C. For $scCO_2$ as the working fluid, the conversion is via direct turbine expansion, with two stages of cooling prior to reaching inlet conditions. To realize commercial-scale thermal and electrical power production levels with CLGSs long borehole lengths are required, making drilling costs a key component of the CAPEX in Eq. (2). Color contour plots of LCOH and LCOE versus mass flow rate (mdot) and horizontal extent (L1) are shown for two drilling costs, expressed as $/m of borehole length, for the u-shaped and coaxial configurations, and water and $scCO_2$ working fluids in Figs. 14 through 16, for a HDR geothermal reservoir. Fixed parameters for these plots were: L1 (depth bgs) = 3500 m, grad = 0.07˚C/m, D = 0.35 m, T_i = 50˚C, k_rock = 3.0 W/m K, r = 7%, n = 40 yr, $O_t = 0.015\ C_t$, and C_t = $100/kWth or C_t = $3000/kWe, which are representative of HDR geothermal reservoirs within the continental United States. Trends of minima in LCOH and LCOE for the four combinations of working fluids and configurations are plotted in Fig. 18, using three drilling costs (100, 500, and 1500 $/m).

Levelized costs for producing heat for direct use (i.e., LCOH) decrease with increasing mass flow rate and horizontal length for the u-shaped configuration, with no minimum identified for both the water or $scCO_2$ working fluid scenarios (Figs. 14 and 15) and are approximately linearly correlated with drilling costs. It's important to note, however, that although higher mass flow rates yield higher produced thermal power, the outlet temperatures decrease with mass flow rate, and minima in LCOH may occur for outlet temperatures with little heating value. For the coaxial configuration, minimums in LCOH occur at intermediate mass flow rates, for both the water or $scCO_2$ working fluid scenarios (Figs. 14 and 15), as lower rates yield lower produced thermal power and higher rates suffer from increased pumping costs, due to pressure drops associated with small hydraulic diameters. As opposed to u-shaped configurations where "more is better" (longer horizontal wells, higher flow rates), coaxial systems need to find the "sweetspot" of well length and flow rate for the most

economic mode of operation. Levelized costs for generating electricity (LCOE) from the produced thermal energy demonstrate the nonlinearities in the LCOE equation, Eq. 2, where lower mass flow rates yield lower LCOEs for lower drilling costs, for both the water or $scCO_2$ working fluid scenarios (Figs. 16 and 17). Reductions in LCOE are realized either through reducing the costs (numerator) or increasing the electricity generated (denominator). Most of the nonlinearities are associated with the denominator term, as the electricity generated is a nonlinear function of flow rate and outlet temperature. As with the LCOH, minima in LCOE for the coaxial configuration occur at intermediate flow rates, for both the water or $scCO_2$ working fluid scenarios (Figs. 16 and 17), as lower rates yield lower produced thermal power and higher rates suffer from increased pumping costs, due to pressure drops associated with small hydraulic diameters. The clipped corners (i.e., high flow rate and low horizontal length) in Fig. 17 occur when the production temperature was getting too low to efficiently make power with the direct turbine expansion cycle. For the turbine outlet pressure chosen (81 bar), the CO2 turbine outlet temperature was getting too close to the critical temperature and the algorithm sets the electricity output to zero for these cases. Increasing the turbine outlet pressure would remove this issue but significantly hurts the electricity output and results in large LCOEs. For the range of horizontal extents and mass flow rates, minima in LCOH and LCOE are approximately linear with drilling costs for all four combinations of system configurations and working fluids (Fig. 18).

An asset of the HDF5 database and associated economic scripts is that LCOH and LCOE minima can be identified and quantified across the domain space (i.e., system configurations, working fluids, and seven independent parameters). These minima are shown in Table 2. Notables in this table are that mass flow rates are not always the parameter-space maximum of 100 kg/s, as higher outlet temperatures yield increases in heat-to-electricity conversion efficiency, and pressure drop across the system can be limiting. Somewhat equivalently, horizontal lengths are not always the parameter-space maximum of 20 km, principally due to pressure drops. Higher injection temperatures are preferred for electricity generation, as these yield higher outlet temperatures, but conversely lower inlet temperatures increase heat transfer rates for direct-use (i.e., heating) scenarios. As anticipated the parameter-space maximums for the geothermal gradient and borehole diameter are always selected. Finally heat-to-electricity conversion efficiencies for these LCOE minima are roughly 15% for water as the working fluid, and 20% for $scCO_2$ as the working fluid. The Utah FORGE project (Utah, 2023) has been achieving record-breaking drilling rates, by employing advanced technologies, such as "physics-based drilling," which incorporates real-time monitoring, evaluating, and mechanical specific energy calculations. With these technologies drilling rates of 7 m/hr in hot granitic rock have been achieved. Industrial costs for drilling geothermal systems are not well published, but Thorhallsson and Sveinbjornsson (2012) did publish on drilling costs for the Hengill field in Iceland. This study reported average drilling rates of 3 m/hr for the deepest sections (i.e., 800 to 2,175 m (bgs)) for 50 boreholes, at an average time cost of $800/m, representing 35.2% of the overall costs, for an overall cost of $2260/m. Using the drilling rate realized at Utah FORGE, this would equal an overall drilling cost of approximately $1000/m ($305/ft) (Table 2).

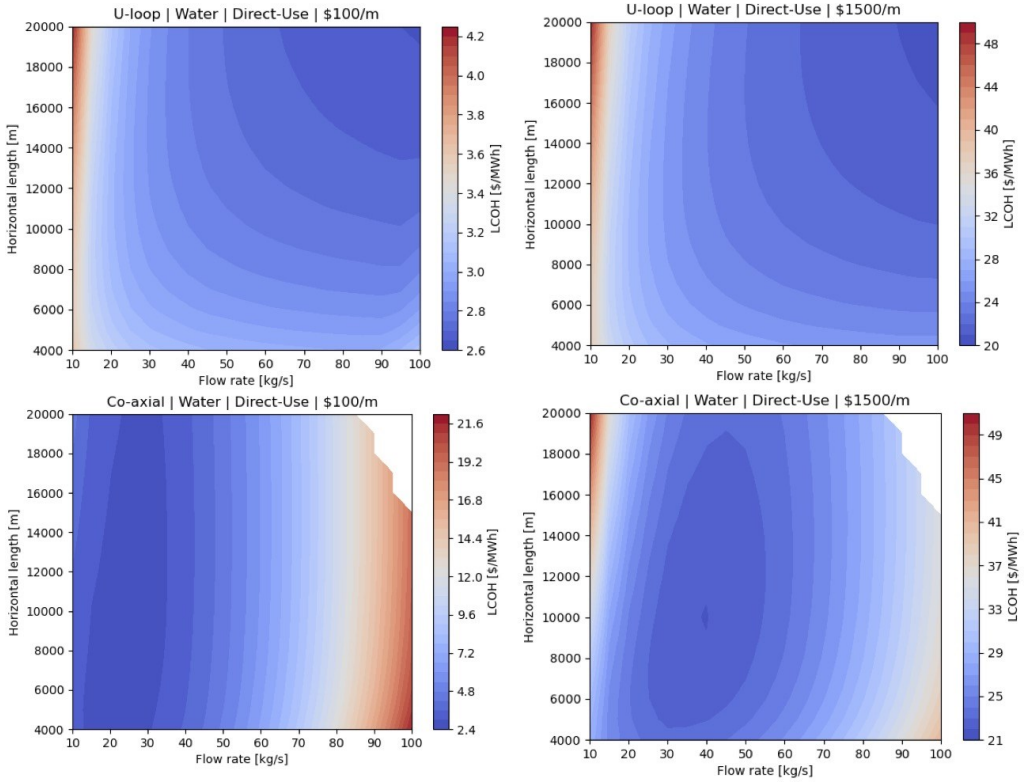

Figure 14: (upper panels) LCOH for u-shaped configuration, water working fluid and (lower panels) coaxial configuration, water working fluid at drilling costs of $100/m and $1500/m. Blank regions in coaxial configuration (lower panels) are excessive pressure drops across the inlet and outlet.

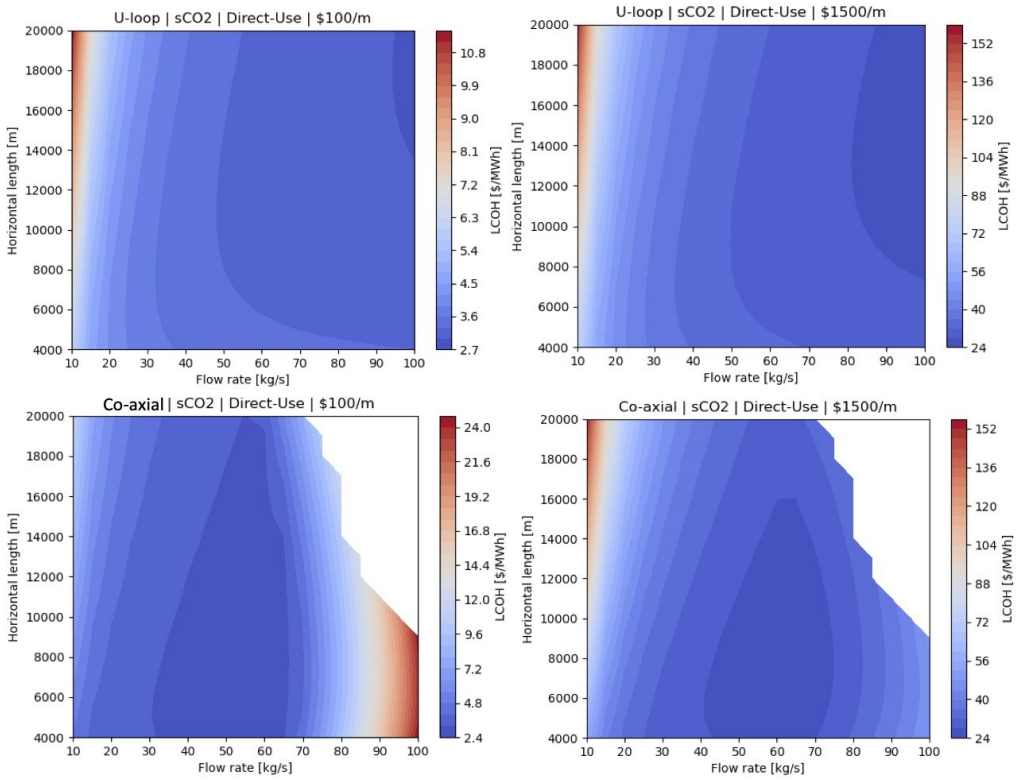

Figure 15: (upper panels) LCOH for u-shaped configuration, $scCO_2$ working fluid and (lower panels) coaxial configuration, $scCO_2$ working fluid at drilling costs of $100/m and $1500/m. Blank region sin coaxial configuration (lower panels) are excessive pressure drops across the inlet and outlet.

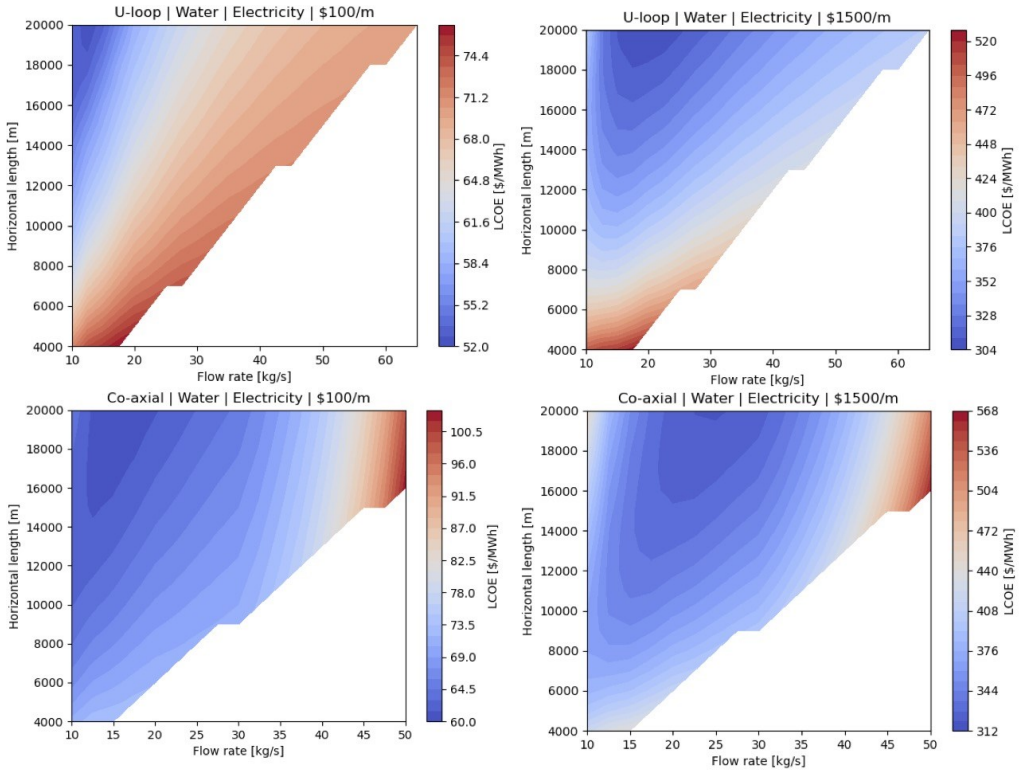

Figure 16: (upper panels) LCOE for u-shaped configuration, water working fluid and (lower panels) coaxial configuration, water working fluid at drilling costs of $100/m and $1500/m. Blank regions in both configurations are outlet temperatures below 100˚C.

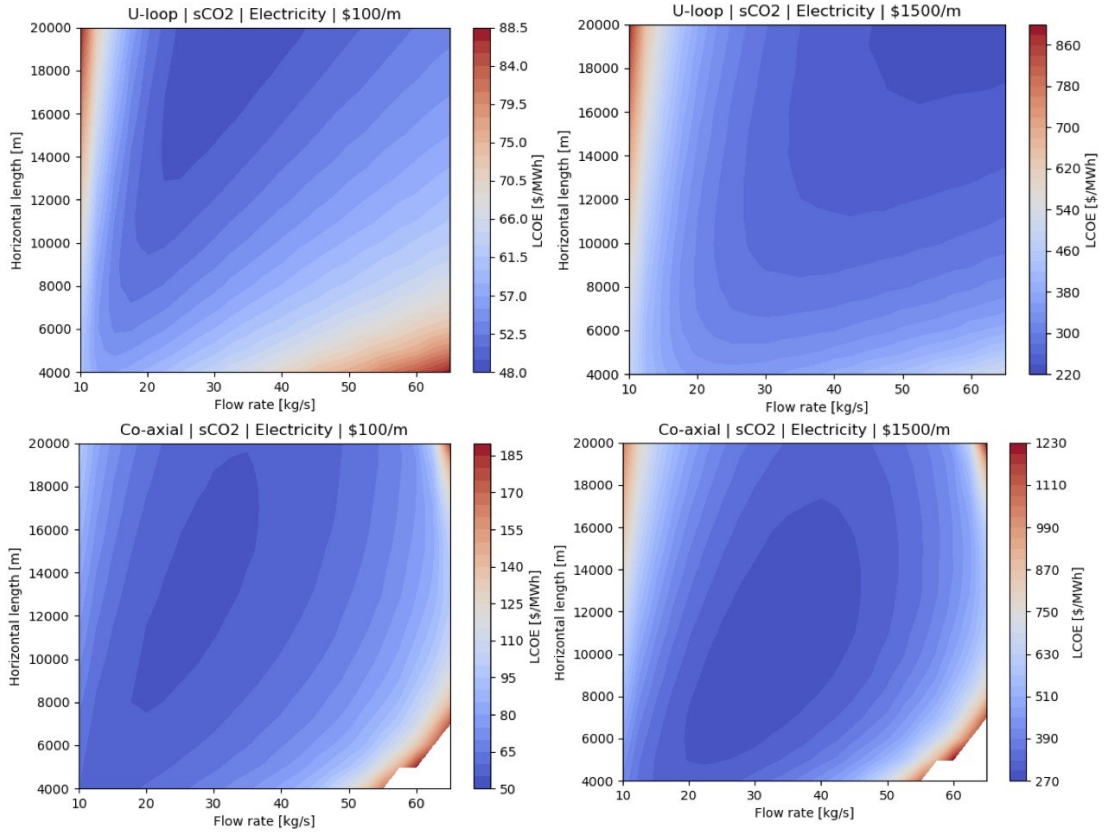

Figure 17: (upper panels) LCOE for u-shaped configuration, $scCO_2$ working fluid and (lower panels) coaxial configuration, $scCO_2$ working fluid at drilling costs of $100/m and $1500/m. Blank regions in coaxial configuration (lower panels) occur when the outlet temperature falls below a conversion efficiency limit for the direct turbine expansion cycle.

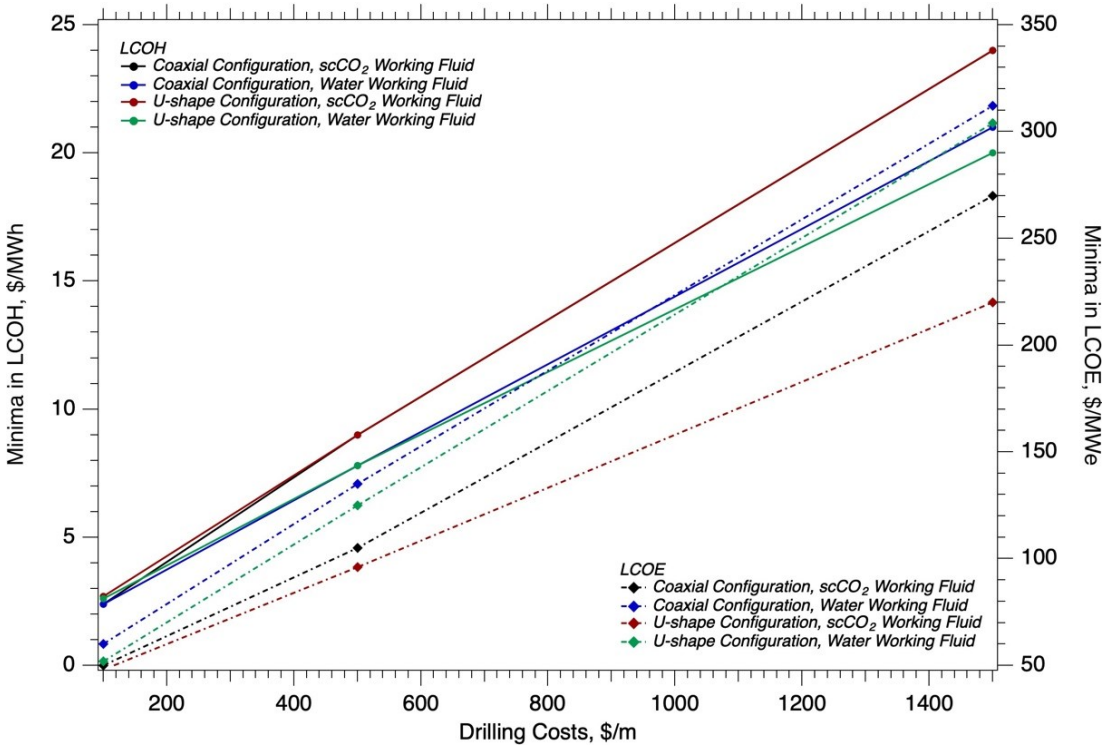

Figure 18: Trends in LCOH and LCOE minima versus drilling costs for the four combinations of configurations and working fluids, with points showing drilling costs of $100/m, $500/m, and $1500/m.

Table 2: Minimum LCOH and LCOE values for the entire domain space (i.e., system configurations, working fluids, and seven independent parameters), for a fixed lifetime of 40 yr, fixed discount rate of 7%, fixed drilling cost of $1000/m, fixed rock thermal conductivity (k) of 4.5 W/m K, fixed depth (L1) of 5,000 m (bgs), geothermal gradient (grad) of 0.07 ˚C/m, and fixed borehole diameter (D) of 0.4445 m (17.5").

System Configuration	U-shaped				Coaxial			
Working Fluid	Water		$scCO_2$		Water		$scCO_2$	
End Use	Heating	Electricity	Heating	Electricity	Heating	Electricity	Heating	Electricity
Mass Flow Rate, kg/s (mdot)	100	43	100	100	73.4	39.2	69.6	69.6
Horizontal Extent, m (L2)	20,000	20,000	11,000	20,000	13,000	20,000	6,000	13,000
Injection Temperature, ˚C (T_i)	30	60	45	60	30	60	45	60
Average Heat Production, MW_{th}	37.4	26.0	17.7	22.2	24.0	23.8	10.2	14.1
Average Electricity Generation, MW_e	-	3.9	-	5.0	-	3.5	-	2.8
Turbine Outlet Pressure, MPa	-	-	-	8.1	-	-	-	8.1
Pre-compression Cooling, ˚C	-	-	-	32	-	-	-	27
LCOH, $/$MWh_{th}$	7.4	-	10.0	-	7.0	-	9.4	-
LCOE, $/$MWh_e$	-	96.6	-	83.0	-	93.5	-	86.9

5. SYSTEM ENHANCEMENTS

Closed-loop geothermal systems in hot-dry-rock (HDR) reservoirs are solely dependent on thermal conduction to transfer heat from the rock to the working fluid. Geothermal reservoirs with permeability (i.e., hot-wet-rock (HWR), such as hot sedimentary basins) have the potential to augment conduction heat transfer with advective heat transfer via natural convection across the borehole, induced by the density changes in the reservoir fluid with temperature. A limited study was conducted, in conjunction with the overall study, that explored the relationship between intrinsic permeability and the performance of CLGSs. The parameter space of this study was much reduced from the hot-dry-rock analysis because of the higher computational demands of fully discretizing the nearby formation around a borehole to simulate convection currents induced by the heat extraction. A u-shaped configuration was considered, with a computational domain that comprised 2.5 km descending and ascending wells with axisymmetric heat conduction with the formation, connected to a lateral borehole embedded in a permeable parallelepiped domain measuring 4 km x 250 m x 250 m. Fixed parameters included a rock conductivity of 3.05 W/m K, local geothermal gradient of 0.07˚C/m, injection temperature of 30˚C, mass flow rate of 15 kg/s, and horizontal length of 4 km. A comparison of the available (exergy) electrical power generated over a 25-year period between permeable (HWR) and impermeable (HDR) reservoirs for two borehole diameters is shown in Fig. 19. The power production for the HDR reservoir displays the classical decline curves for conduction-dominated systems, whereas those for HWR reservoir show gradual decreases over time, as the heat resource becomes depleted. The temporal development of the convection plume is shown in a slice orthogonal to the borehole in Fig. 20. Borehole surface area plays a similar, though enhanced role, in permeable systems to that in HDR systems. A 500 mD layer increases the power output over conduction (HDR) by roughly 2x and by about 3x in a 2000 mD layer. For example, a 4 MWe plant would require roughly 4 – 4km laterals in a 2000 mD layer compared to about 12 laterals in HDR.

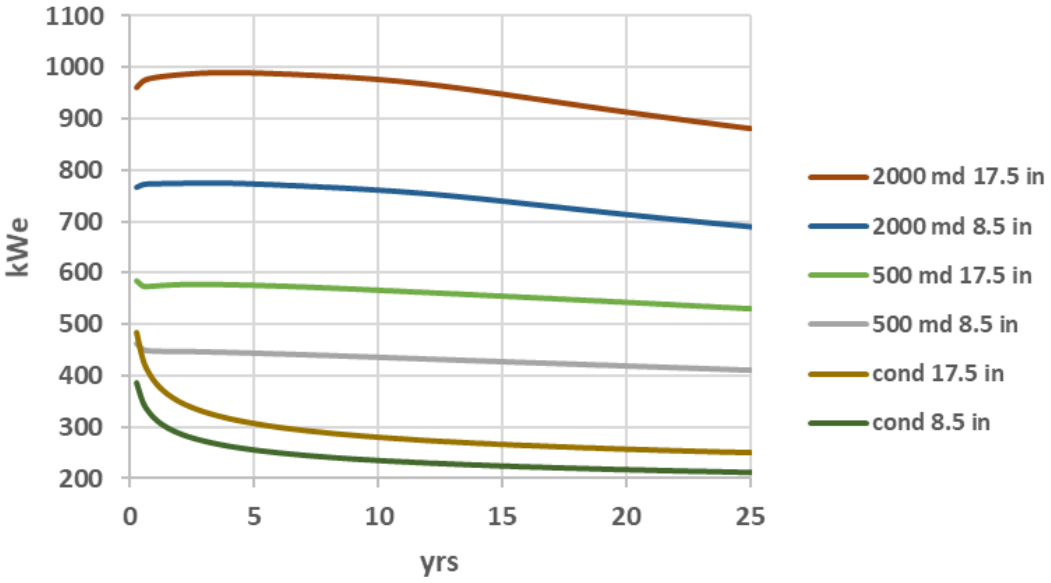

Figure 19: Available electrical power as a function of reservoir permeability, and tubing diameter (8.5 and 17.5 inch) in a closed-loop u-tube sited at 2.5 km depth (bgs) with 4 km lateral circulating water at 15 kg/s. Curves for the corresponding HDR simulations (conduction heat transfer in the formation) are labelled "cond."

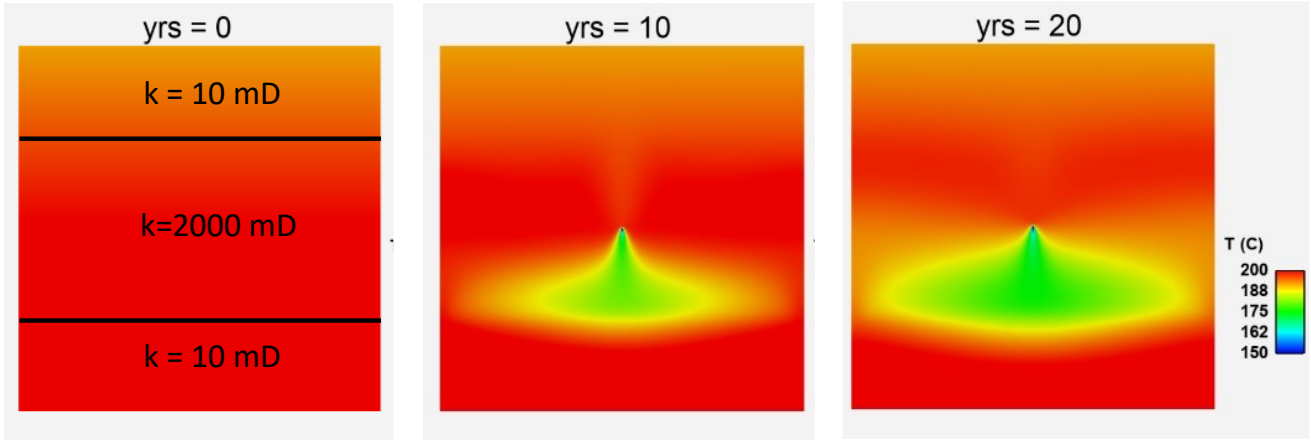

Figure 20: Cold plume temporal development in a vertical plane (250m x 250 m) midway (2 km from inlet to lateral) along a 4 km lateral sited in a 2 D hot wet reservoir. The permeable reservoir occupies the central 125 m height of the domain.

One engineering solution to the low thermal conductivity of the reservoir rock would be to over drill the borehole and then fill the annular space between the outer borehole wall and rock with highly conductive material. As with the natural convection study, a limited study was conducted in conjunction with the overall study to understand the potential of this approach, without consideration of costs. This study used a modified version of the SNL axisymmetric models for the 10-km u-shaped (Fig. 21) and coaxial configurations and first considered an annular thickness of 1 m and thermal conductivity of 10 W/m K, and then considered annular thickness from 1 to 10 m and thermal conductivity from 10 to 100 W/m K. One caveat concerning this study is that we assumed that the annular fill material had reached equilibrium temperatures with the rock prior to starting the working fluid circulation. For the first scenario, modest temperature increases after 40 years of production were realized for the coaxial configuration (i.e., 56.2 to 64.8˚C) and for the u-shaped configuration (i.e., 137.9 to 156.2˚C). For the second scenario, energy recovery (exergy based) after 40 years for an annular fill thickness of 1 m and thermal conductivity of 10 W/m K, increased by a factor of 1.4 and at the extreme annular thickness of 10 m and thermal conductivity of 100 W/m K only increased by a factor of 2.3.

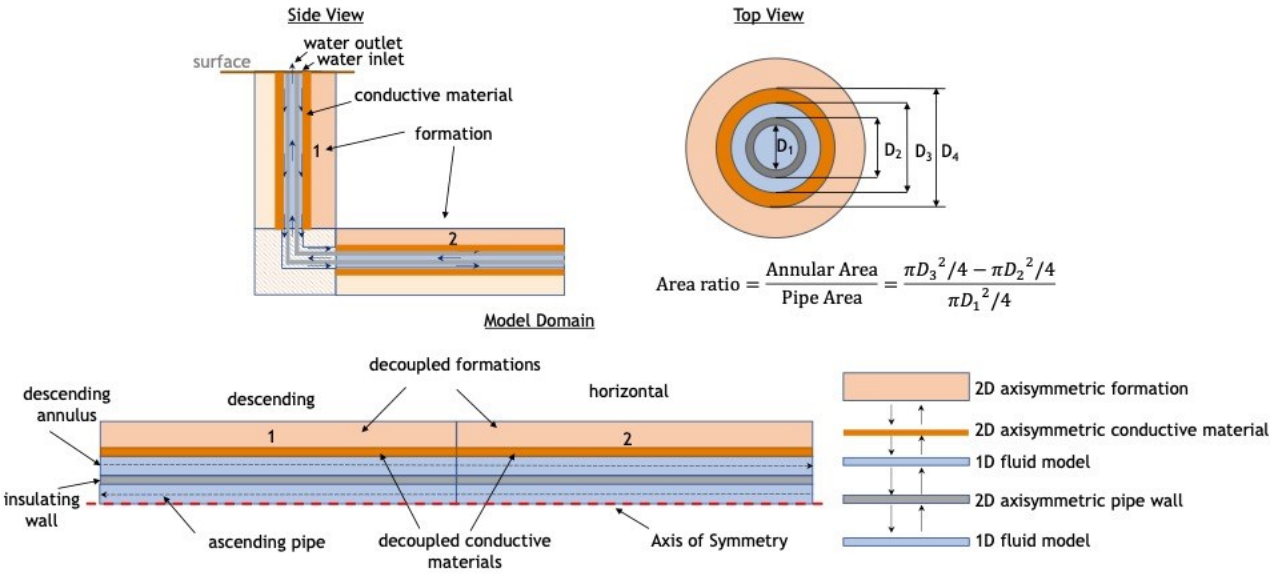

Figure 21: Modified SNL axisymmetric model for the coaxial configuration with conductive material between the inner pipe and borehole wall.

A second engineering solution would be to increase the effect subsurface heat exchanger area via fractures. Wang et al. (2010) investigated the potential of coupling a coaxial configuration with overlapping vertically oriented fractures. The concept behind this configuration was to minimize drilling costs by developing a single-well enhanced geothermal system (EGS) in nominally impermeable rock. This design would allow for water to be the working fluid within the fracture network, and a separate working fluid to circulate in the coaxial system, thus potentially eliminating the fouling and dissolution difficulties of more conventional two-well EGS reservoirs. Fluid circulation in the fracture network was assumed to occur via natural circulation, and in the coaxial system via natural circulation with pumping assist if needed to overcome flow resistance. This numerical study found $scCO_2$ to have advantages over other organic fluids, such as isopentane. This binary fluid system yielded heat production levels of 0.5 MW_{th} and electricity generation levels of 0.05 MW_e, principally due to the limited flow rates of the water circulating in the fracture network. To overcome these uneconomical heat production levels, the study further considered forcing circulation of fluid directly from the coaxial system through the fracture network, yielding a single working fluid. Again $scCO_2$ had advantages as the working fluid with respect to thermal extraction and electricity generation, and losses to the subsurface environment had the potential of being beneficial with respect to carbon sequestration. This design did show some merits with heat production levels of 35 MWth for water as the working fluid, but the direct contact with the rock eliminates this design from the classification of CLGSs.

6. CONCLUSIONS

The United States Department of Energy (DOE), Geothermal Technologies Office (GTO) sponsored an independent investigation of closed-loop geothermal systems (CLGSs) to understand the potential and limitations of producing thermal energy from geothermal reservoirs with marginal working fluid losses and to assess the net average present cost of using the produced heat directly or using it to generate electricity. This investigation, known as the Closed Loop Geothermal Working Group, was a collaborative numerical study involving teams of scientists and engineers from four national laboratories, plus expert panel members. The study first demonstrated the ability of independent numerical simulators to model CLGSs, by comparing against existing field data, analytical solutions, and code intercomparisons. The study additionally demonstrated the validity of the axisymmetric modeling approach, thus establishing a computationally efficient approach for modeling complex CLGSs. The study then used a version of the axisymmetric modeling approach to develop a thermal performance database, stored in HDF5 format, for two configurations (i.e., u-shaped and coaxial) and two working fluids (i.e., water and $scCO_2$) for a hot-dry-rock (HDR) geothermal reservoir, limited to temperatures below the critical point of water (i.e., 374˚C). The database is structured by working fluid, system configuration, seven variable parameters, and contains outlet temperature and pressure tabulated quarterly (i.e., 161 points) over a time period from 0 to 40 years for each of the 2,527,200 combinations of fluids, configurations, and parameters. Established power plant models and cost correlations were then linked to the database via Python scripts to estimate electricity generation output and overall levelized cost of electricity (LCOE) and heat (LCOH). To make this database and cost correlations readily accessible to the public an interface was developed and posted on the Geothermal Data Repository (GDR) (url).

The reality of the thermal performance potential of CLGSs was realized by the early analytical work of Ramey (1962) for u-shaped configurations and Horne (1980) for coaxial configuration. These investigations demonstrated that long-term heat recovery was controlled by rock thermal conductivity and to overcome the low intrinsic thermal conductivity of rock large surface area would be required to recover heat at the commercial scale (i.e., > 5 MWth). The independent investigations of this study reinforce this finding for both u-shaped and coaxial configurations and water and $scCO_2$ working fluids (i.e., regardless the engineering, the intrinsic poor thermal conductivity of rock controls the long-term thermal performance of CLGSs). Surface area for CLGSs is determined by borehole diameter and total borehole length over the region where rock temperatures are greater than the working fluid temperature. A reasonable upper limit for

borehole diameters using conventional drilling techniques would be around 17.5 in (0.4445 m), thus borehole extent within the geothermal reservoir is principal approach for increasing surface area. The analytical solutions developed by Ramey (1962) and Horne (1980), which concur with the findings of this study, noted that heat production is directly correlated with mass flow rate, but that increasing mass flow rate has two detriments: decreasing outlet temperature and increasing pumping cost (if no longer buoyancy driven). For direct-use applications there are utility limits with respect to outlet temperature and for electricity generation the efficiency of thermal to mechanical energy conversion is nonlinearly correlated with outlet temperature. As with rock thermal conductivity, low outlet temperatures can be overcome with surface area, which requires increasing the borehole extent within the geothermal reservoir proper. Whereas this study has demonstrated the potential for producing heat with CLGSs at the commercial scale (i.e., > 5 MW), the commercial viability of CLGSs must carefully be considered.

The study highlighted the fundamental behavior of CLGS. One of the key characteristics of CLGS is that the outlet temperature versus time plots follow a specific behavior – a transient period, early in time, with a sharp decline in temperature, followed with a slower decline in temperature. Another key characteristic of CLGS is that the production temperature is significantly lower than the rock reservoir temperature for most of its life. Both characteristics stem from conduction through reservoir rock being the dominant heat transfer mechanism in CLGS. The physical behavior of CLGS is well understood and there are limited steps that can be taken to increase thermal and useful energy output, the primary one being to increase the surface of the CLGS in contact with the rock reservoir. This is usually achieved by either making the borehole longer and/or increasing its diameter. Both normally come at an increased capital cost. Even under the most favorable conditions, CLGS wells tend to have energy output that is comparable and usually less than that from a typical conventional hydrothermal well. The main factor in CLGS project economics is the cost of drilling and completing the CLGS, and whether the energy production justifies the drilling expense.

The current U.S. average for energy content of natural gas, as reported by the U.S. Energy Information Administration (EIA), is around 1030 MBtu/MCF (302 kWh/MCF), and the current industrial price for natural gas, as reported by the EIA, varies but \$8/MCF is representative, yielding an industrial heating cost of \$0.0265/kWh_{th} (\$26.5/MWh_{th}). For a water working fluid, LCOH values near or below this range are possible for drilling costs of \$1500/m and below, as shown in the economic analysis section, for a representative CLGS. Additionally, for LCOH values within this range, outlet temperatures for the u-shaped and coaxial configurations after 40 years above 90 and 85˚C are possible, respectively. Average produced heat values for these CLGSs are 9.8 MW_{th} at 50 kg/s for the u-shaped configuration and 8.9 MW_{th} at 40 kg/s for the coaxial configuration. For a $scCO_2$ working fluid, the range of mass flow rates and horizontal extents is more limited than those for water to realize LCOH levels below \$26.5/MWh_{th}, but achievable, and outlet temperatures for the u-shaped and coaxial configurations after 40 years above 85 and nearly 90˚C are possible, respectively. Average produced heat values for these CLGSs are 7.8 MW_{th} at 85 kg/s for the u-shaped configuration and 6.8 MW_{th} at 60 kg/s for the coaxial configuration. To understand the heat recovery and LCOH of specific CLGSs the interface or Python scripts posted on the GDR (url) are recommended.

https://gdr.openei.org/submissions/1473

The current U.S. average cost for electricity for the industrial sector, as reported by the U.S. Energy Information Administration (EIA), is \$86.1/MWhe. In the domain space considered and with a drilling cost of \$1,000/m, the lowest LCOE found with water as heat transfer fluid was around \$94/MW_e for a co-axial configuration with 0.4445 m borehole, 20,000 m horizontal length, 5,000 m depth (bgs), 4.5 W/m K rock thermal conductivity, and 70°C/km geothermal gradient. Similarly, for scCO2 as the working fluid, the lowest LCOE found for the domain space considered and a \$1,000/m drilling cost was \$83/MW_e. This system was a U-loop configuration with 0.4445 m borehole, 20,000 m horizontal length, 5,000 m depth (bgs), 4.5 W/m K rock thermal conductivity, and 70°C/km geothermal gradient, and produced about 22 MW_{th} of heat, converting into about 5 MW_e of electricity. Note that a gradient of 70°C/km and rock thermal conductivity of 4.5 W/m K are on the upper end of the spectrum of the geothermal resource base, so that these assumptions could be called an optimistic scenario. While the domain space considered includes a wide range of systems proposed by developers and found in literature, not all designs are covered, and some may result in different performance than found for the systems presented in this paper. For example, some closed-loop developers focus on repurposing abandoned wells and hereby avoid drilling new wells, generally the highest expense of a greenfield system. As with direct-use applications of the produced heat from CLGSs, to understand the electricity generation potential and LCOE of specific CLGSs the interface or Python scripts posted on the GDR are recommended.

https://gdr.openei.org/submissions/1473

ACKNOWLEGEMENTS

This material was based upon work supported by the U.S. Department of Energy, Office of Energy Efficiency and Renewable Energy (EERE), Office of Technology Development, Geothermal Technologies Office, under Award Number DE-AC05-76RL01830 with PNNL and other awards to other national laboratories. The United States Government retains, and the publisher, by accepting the article for publication, acknowledges that the United States Government retains a non-exclusive, paid-up, irrevocable, world-wide license to publish or reproduce the published form of this manuscript, or allow others to do so, for United States Government purposes. This work is guided by an expert panel comprising Roland Horne (Stanford University), Laura Pauley (Pennsylvania State University), and Chad Augustine (National Renewable Energy Laboratory). We recognize and appreciate their dedication to the study and have greatly benefitted from their suggestions and reviews of the work.

REFERENCES

Barker, B.J., Gulati, M.S., Bryan, M.A., Riedel, K.L.: Geysers Reservoir Performance. Monograph on the Geysers Geothermal Field, Special Report No. 17, Geothermal Resources Council, (1991), 167–177.

Beckers, K.F., Rangel-Jurado, N., Chandrasekar, H., Hawkins, A.J.. Fulton, P.M., Tester, J.W.: Techno-Economic Performance of Closed-Loop Geothermal Systems for Heat Production and Electricity Generation, Geothermics 100 (2022), doi 10.1016/j.geothermics.2021.102318.

Beckers, K.F., Vasyliv, Y., Bran-Anleu, G.A., Martinez, M., White, M.D.: Tabulated Database of Closed-Loop Geothermal Systems Performance for Cloud-Based Technical and Economic Modeling of Heat Production and Electricity Generation, Proceedings of the 48th on Geothermal Reservoir Engineering, (2023) Stanford University, Stanford, CA, SGP-TR-224.

Bell, I. H., Wronski, J., Quoilin, S., & Lemort, V. (2014). Pure and Pseudo-pure Fluid Thermophysical Property Evaluation and the Open-Source Thermophysical Property Library CoolProp. Industrial & Engineering Chemistry Research, 53(6), 2498-2508. https://doi.org/10.1021/ie4033999

Brown, D.W., Duchane, D.V., Heiken, G., Hriscu, V.T.: Mining the Earth's Heat: Hot Dry Rock Geothermal Energy, Springer, (2012), ISBN 978-3-540-67316-3, doi 10.1007/978-3-540-68910-2.

Bodvarsson, G.S., Pruess, K., Lippmann, M.J.: Modeling of Geothermal Systems, Lawrence Berkeley Laboratory, (1985), LBL-18268.

Dalbey, K., Eldred, M. S., Geraci, G., Jakeman, J. D., Maupin, K. A., Monschke, J. A., Seidl, D. T., Swiler, L. P., Tran, A., & Menhorn, F. (2020). Dakota A Multilevel Parallel Object-Oriented Framework for Design Optimization Parameter Estimation Uncertainty Quantification and Sensitivity Analysis: Version 6.12 Theory Manual. SAND2020-4987, Sandia National Laboratory.

Gnielinski, V.: Neue Gleichungen für den Wärme- und den Stoffübergang in turbulent durchströmten Rohren und Kanälen. Forsch. Ing.-Wes., 41(1), 8-16, (1975).

Hagoort, J.: Ramey's Wellbore Heat Transmission Revisited, SPE Journal, 9(04), (2004), 465-474, SPE-87305-PA, doi: 10.2118/87305-PA

Horne, R.N.: Design Considerations of a Down-Hole Coaxial Geothermal Heat Exchanger, Geothermal Resources Council, Transactions, 4, (1980), 569-572.

Incropera, F.P., DeWitt, D.P.: Fundamentals of Heat and Mass Transfer (6th ed.), (2007), Hoboken, Wiley.

Morita, K., Bollmeier, W.S., Mizogami, H.: Analysis of the results from the downhole coaxial heat exchanger (DCHE) experiment in Hawaii, Geothermal Resources Council Transactions, 16, (1992a), 9-16.

Morita, K., Bollmeier, W.S., Mizogami, H.: An experiment to prove the concept of the downhole coaxial heat exchanger (DCHE) experiment in Hawaii, Geothermal Resources Council Transactions, 16, (1992b), 17-23.

Nalla, G., Shook, G.M., Mines, G.L., Bloomfield, K.K.: Parametric sensitivity study of operating and design variables in wellbore heat exchangers, Geothermics, 34, (2005), 330-346, doi:10.1016/j.geothermics.2005.02.001.

Novak, A.J., Carlsen, R.W., Schunert, S., Balestra, P., Reger, D., Slaybaugh, R.N, Martineau, R.C.: Pronghorn: A Multidimensional Coarse-Mesh Application for Advanced Reactor Thermal Hydraulics, Nuclear Technology, 207, (2021), 1015-1046, doi 10.1080/00295450.2020.1825307.

Oostrom, M., White, M.D.: STOMP Subsurface Transport Over Multiple Phases Version 3.1 User's Guide, PNNL-14286, (2004), Pacific Northwest National Laboratory.

Parisi, C., Balestra, P., Marshall, T.D.: Geothermal Analysis Modeling and Simulation Using Idaho National Laboratory' RELAP5-3D-PRONGHORN Coupled Codes, Geothermal Resources Council, Transactions, 45 (2021).

Parisi, C., Balestra, P., Kyanjo, B., Marshall, T.D., McLing, T.L.: Closed Loop Geothermal Analysis Modeling and Simulation Using Idaho National Laboratory's RELAP5-3D-FALCON Coupled Codes, Proceedings of the 48th on Geothermal Reservoir Engineering, (2023) Stanford University, Stanford, CA, SGP-TR-224.

Podgorney, R.K., Finnila, A., Ghassemi, A., McLennan, J., Moore, J.: Reference Native State and Stimulation Models of the Utah FORGE Site, Proceedings of the 45th Workshop on Geothermal Reservoir Engineering, (2020), Stanford University, Stanford, CA, SGP-TR-216.

Ramey, H.J.: Wellbore Heat Transmission, Transactions of the Society of Petroleum Engineers, 225(4), (1962), 427-435, SPE-00811696.

RELAP5-3D Code Development Team, "RELAP5-3D Code Manual Volume I: Code Structure, System Models and Solution Methods", Idaho National Laboratory, INL/MIS-15-36723, rev. 4.4., Idaho Falls, ID (2018a).

RELAP5-3D Code Development Team, "RELAP5-3D Code Manual Volume IV: Models and Correlations.", Idaho National Laboratory, INL/MIS-15-36723, rev. 4.4, Idaho Falls, ID (2018b).

Robertson, E.C.: Thermal Properties of Rocks, United States Department of the Interior Geological Survey, Open-File Report 88-441 (1988), Reston, Virginia.

Shu, J.: Comparison of Various Techniques for Computing Well Index, (2005), Stanford University, Stanford, CA.

Sierra Thermal Fluid Development Team: SIERRA Multimechanics Module: Aria User Manual – Version 4.56, Sandia National Laboratory, SAND-2020-4000 685399, (2020), doi 10.2172/1615880.

Thorhallsson, S., Sveinbjornsson, B.M.: Geothermal Drilling Cost and Drilling Effectiveness, (2012), Presented at "Short Course on Geothermal Development and Geothermal Wells," organized by United Nations University-Geothermal Training Programme and LaGeo S.A. de C.V., in Santa Tecla, El Salvador, March 11-17, 2012.

Vasyliv, Y., Bran-Anleu, G.A., Kucala, A., Subia, S., Martinez, M.: Analysis and Optimization of a Closed Loop Geothermal System in Hot Rock Reservoirs, Geothermal Resources Council, Transactions, 45 (2021).

Utah FORGE: At the Core, Utah FORGE Newsletter, April (2021), Accessed January 16, 2023, https://utahforge.com/wp-content/uploads/sites/96/2021/04/Newsletter5-1.pdf

Wang, Z., McClure, M.W., Horne, R.N.: Modeling Study of Single-Well EGS Configurations, (2010), Proceedings of World Geothermal Congress, 2010, Bali, Indonesia, 25-29 April 2010.

White, M.D., Bacon, D.H., White, S.K., Zhang, Z.F.: Fully Coupled Well Models for Fluid Injection and Production, Energy Procedia, 37, (2013), 3960-3970.

White, M.D., Fu, P., EGS Collab Team: Application of an Embedded Fracture and Borehole Modeling Approach to the Understanding of EGS Collab Experiment 1, Proceedings of the 44th Workshop on Geothermal Reservoir Engineering, (2019), Stanford University, Stanford, CA, SGP-TR-215.

White, M.D., Martinez, M., Vasyliv, Y., Bran-Anleu, G.A., Parisi, C., Balestra, P., Horne, R.N., Augustine, C., Pauley, L., Hollett, D., Bettin, G., Marshall, T. and the Closed Loop Geothermal Working Group: Thermal and mechanical energy performance analysis of closed-loop systems in hot-dry-rock and hot-wet-rock reservoirs, Geothermal Resources Council, Transactions, 45 (2021).